

THIS REPORT HAS BEEN DELIMITED  
AND CLEARED FOR PUBLIC RELEASE  
UNDER DOD DIRECTIVE 5200.20 AND  
NO RESTRICTIONS ARE IMPOSED UPON  
ITS USE AND DISCLOSURE.

DISTRIBUTION STATEMENT A

APPROVED FOR PUBLIC RELEASE;  
DISTRIBUTION UNLIMITED.

# Armed Services Technical Information Agency

Because of our limited supply, you are requested to return this copy WHEN IT HAS SERVED YOUR PURPOSE so that it may be made available to other requesters. Your cooperation will be appreciated.

# AD

# 40603

NOTICE: WHEN GOVERNMENT OR OTHER DRAWINGS, SPECIFICATIONS OR OTHER DATA ARE USED FOR ANY PURPOSE OTHER THAN IN CONNECTION WITH A DEFINITELY RELATED GOVERNMENT PROCUREMENT OPERATION, THE U. S. GOVERNMENT THEREBY INCURS NO RESPONSIBILITY, NOR ANY OBLIGATION WHATSOEVER; AND THE FACT THAT THE GOVERNMENT MAY HAVE FORMULATED, FURNISHED, OR IN ANY WAY SUPPLIED THE SAID DRAWINGS, SPECIFICATIONS, OR OTHER DATA IS NOT TO BE REGARDED BY IMPLICATION OR OTHERWISE AS IN ANY MANNER LICENSING THE HOLDER OR ANY OTHER PERSON OR CORPORATION, OR CONVEYING ANY RIGHTS OR PERMISSION TO MANUFACTURE, USE OR SELL ANY PATENTED INVENTION THAT MAY IN ANY WAY BE RELATED THERETO.

Reproduced by  
**DOCUMENT SERVICE CENTER**  
KNOTT BUILDING, DAYTON, 2, OHIO

# UNCLASSIFIED

AD No. **40603**  
ASTIA FILE COPY

Office of Naval Research

---

Contract N50RI-76 • Task Order No.1 • NR-071-012

NUCLEAR MAGNETIC RESONANCE IN IMPERFECT CRYSTALS



By

N. Bloembergen

June 18, 1954

Technical Report No. 199

---

Craft Laboratory  
Harvard University  
Cambridge, Massachusetts

Office of Naval Research

Contract N5ori-76

Task Order No. 1

NR-071-011

Technical Report

on

Nuclear Magnetic Resonance in Imperfect Crystals

by

N. Bloembergen

June 18, 1954

The research reported in this document was made possible through support extended Cruft Laboratory, Harvard University, jointly by the Navy Department (Office of Naval Research), the Signal Corps of the U. S. Army, and the U. S. Air Force, under ONR Contract N5ori-76, T. O. 1.

Technical Report No. 199

Cruft Laboratory

Harvard University

Cambridge, Massachusetts

## Nuclear Magnetic Resonance in Imperfect Crystals\*

by

N. Bloembergen

Division of Applied Science, Harvard University

Cambridge, Massachusetts

### Abstract

A systematic survey is made how various kinds of imperfections in a crystalline lattice will affect the position, breadth, shape and relaxation time of the nuclear magnetic resonance. In accordance with Seitz's classification the following imperfections are considered: (a) dislocations; (b) vacant lattice sites and interstitial atoms; (c) foreign atoms in either interstitial or substitutional position; (d) electrons and holes; (e) phonons; (f) excitons. Their interaction with the magnetic dipole moment and the electric quadrupole moment of the nuclei at the normal lattice sites is discussed and the available experimental information is reviewed.

### I

#### Introduction

The nature of imperfections in nearly perfect crystals has been studied extensively during the last two decades. An excellent synthesis of this broad field has been given by Seitz [1]. At the time his report was written only one or two connections between crystalline imperfections and nuclear magnetic resonance were known. During the past few years several new examples of the interplay of magnetic resonance phenomena and imperfections in a crystalline lattice have been found. Some of these have recently been reviewed by Pound [2], some others will be discussed in more detail during the Bristol Conference. It may be profitable to give a broad and systematic review of the possible interactions between nuclear spins and lattice imperfections. In

-----  
\*Part of this research was supported jointly by the Office of Naval Research, Army Signal Corps and the U. S. Air Force. This paper contains the material of two lectures presented at the Bristol Conference, July 1954. The author is indebted to the ONR for transatlantic transportation.

the course of this survey the opportunity will arise from time to time to point unsolved problems and directions in which further investigation might be fruitful. Some special attention will be paid to metals and alloys, where conduction electrons and foreign solute atoms cause prominent effects. It is hoped that this review will stimulate further research in a field, the exploration of which seems to be still in its infancy.

According to Seitz the imperfections to be considered can be classified as:

- (a) dislocations
- (b) vacant lattice sites and interstitial atoms
- (c) foreign atoms in either substitutional or interstitial positions
- (d) free electrons and holes
- (e) lattice phonons
- (f) excitons

These imperfections may change the distribution of the internal magnetic fields and the gradients of the crystalline electric field. In Section II the interaction of these imperfections and the nuclear magnetic dipole moments is discussed, and Section III deals with the interaction with the nuclear electric quadrupole moments.

The direct effect of transient imperfections in the form of light quanta, charged and uncharged material radiations is negligible, unless one wishes to consider the radiofrequency field inducing the nuclear spin transitions itself as photons disturbing the lattice.

## II

### Magnetic Dipole Interactions

In diamagnetic crystals the internal magnetic field acting on a nuclear spin consists almost entirely of the contribution from neighboring nuclear magnetic moments. The random spin orientation of these neighbors gives rise to a line broadening of the magnetic resonance line, whose second moment is given by the celebrated formula of Van Vleck [3]

$$\overline{(\delta\nu)^2} = \frac{3}{4} I(I+1) \gamma^4 \hbar^2 \sum_j r_{oj}^{-6} (1 - 3 \cos^2 \theta_{oj})^2 +$$

$$+ \frac{1}{3} \gamma^2 \hbar^2 \sum_j \gamma_f^2 I_f(I_f+1) r_{of}^{-6} (1 - 3 \cos^2 \theta_{of})^2 \quad (1)$$

where the second moment is defined by

$$\overline{(\delta\nu)^2} = \int_0^\infty (\nu - \nu_0)^2 g(\nu) d\nu, \quad \int_0^\infty g(\nu) d\nu = 1,$$

$g(\nu)$  is the normalized shape factor of the absorption line. The first summation on the right-hand side of equation (1) extends over all identical nuclear spins  $j$ , the second sum over all different spins  $f$ . The nuclear gyromagnetic constant  $\gamma$  relates the resonance frequency with the magnetic field

$$2\pi \nu_0 = \gamma H_0, \quad (2)$$

$r_{oj}$  and  $r_{of}$  are internuclear distances and  $\theta$  is the angle between the radius vector and the magnetic field  $H_0$ . The magnetic field acting on the nucleus will be composed of the external field  $H_0$  and the internal or local fields. The dipolar interaction produces random variations from the mean value  $H_0$ , which find their quantitative expression in equation (1).

#### A. Dislocations

In the neighborhood of a dislocation the internuclear distances will have changed somewhat, but usually less than one per cent. The corresponding change in the width of the resonance given by equation (1) is therefore negligible. However, if the nuclei under consideration have a quadrupole moment, a change in the value of the second moment will occur, as will be explained later when the quadrupole effects are discussed.

The contribution of the electron orbitals to the magnetization, which is of course zero for completely filled bands, is usually quenched by the crystalline electric field even for incompletely filled shells. The small change in the crystalline fields due to the strains around a dislocation will not change this situation. In particular, a diamagnetic substance will remain diamagnetic under deformation and the contribution of the electrons to the internal magnetic field at the position of the nuclei in the solid remains negligible.

It is conceivable that an indirect effect may occur in the presence of

paramagnetic ions. The Hamiltonian containing the crystalline field splitting and the spin-orbit coupling of these ions may change, and therefore the relaxation time of the electron spins could be changed in a strained lattice if the symmetry of the crystalline field is lowered by the deformation. This might in turn change the relaxation time of the nuclear spins by a mechanism which will be discussed in paragraph (C). As the influence of deformation on the electron spins in paramagnetic materials has received little attention and as it is only a side issue for the nuclear resonance, we shall not pursue this matter any further.

We arrive at the conclusion that dislocations in general have a negligible influence on the nuclear resonance in the absence of quadrupole effects ( $I = \frac{1}{2}$ ).

#### B. Vacancies and interstitial atoms

The presence of vacancies and interstitial atoms will cause an obvious change in the summations of equation (1). Since their concentration will usually not exceed 1 atomic per cent, the second moment in the static lattice remains practically unchanged.

Nevertheless, vacancies and interstitials can have a pronounced effect on the line width and the spin lattice relaxation time. At sufficiently high temperatures they make diffusion possible and as the individual nuclei carry out diffusion jumps, the internal magnetic field acting on the nuclear spins will have a time dependence with a characteristic time given by

$$\tau^{-1} = \nu_{\text{diff}} = \nu_{\text{at}} \exp \left\{ -(E_{\text{act}} + E_{\text{vac}})/kT \right\} \quad (3)$$

where  $\nu_{\text{at}}$  is a constant of the order of the atomic vibration frequency,  $E_{\text{vac}}$  is the energy for formation of a vacancy or interstitial atom and  $E_{\text{act}}$  is the activation energy necessary to move such a vacancy or interstitial over an atomic distance. Time-dependent internal fields have been discussed by Bloembergen, Purcell and Pound [4] for nuclear relaxation effects in liquids. The same treatment applies to motion in solids.

The line width due to dipolar interaction between randomly moving dipoles with a correlation time  $\tau$  is given by the approximate formula

$$1/T_2 = \delta\nu_{\text{eff}} = \left(\frac{2}{\pi}\right)^{1/2} \overline{(\delta\nu)^2}^{1/2} \left\{ \arctg(2\tau\delta\nu_{\text{eff}}) \right\}^{1/2} \quad (4)$$

and the relaxation time by

$$1/T_1 = K \left( \frac{\tau}{1+4\pi^2\nu_0^2\tau^2} + \frac{2\tau}{1+16\pi^2\nu_0^2\tau^2} \right) \quad (5)$$

In general there will not be a single characteristic time, and a more accurate integration over a distribution of  $\tau$ 's is appropriate. A refined analysis for the diffusional motion and its effect on the nuclear relaxation has been given by Torrey [5]. The effects of diffusional motion in solids on the nuclear spin resonance was first discovered at the University of Illinois in metallic sodium [6], but similar effects will occur in any solid if the diffusion is rapid enough. The main features of equations (4) and (5) are

- (1) When the diffusion jump frequency  $\nu_{\text{diff}}$  becomes larger than the linewidth  $\langle (\delta\nu)^2 \rangle^{1/2}$  of the rigid lattice, a motional narrowing of the line sets in.
- (2) The relaxation time  $T_1$  will pass through a minimum when  $\nu_{\text{diff}}$  is of the order of the Larmor precession frequency  $\nu_0$  of the nuclear spins. By measuring the line width and  $T_1$  as a function of temperature the activation energy for self-diffusion is determined. The diffusion of different isotopes can be studied separately.

A particularly interesting application could be made to ionic crystals, e.g., the alkali and silver halides. The time dependence of the dipolar interaction between two slow-moving anion-nuclei would be determined by the jump frequency of the anions, but the dipolar interaction between cation-anion and cation-cation pairs would have a frequency spectrum determined largely by the higher jump frequency of the cations. For the nuclear resonance of the anions one would have two terms on the right side of equations (4) and (5), one with a longer  $\tau$  for the dipolar interaction between two anions, and one with a shorter  $\tau$  for the anion-cation dipolar interaction. Diffusion effects in solids are discussed in detail in papers by Andrew and Slichter at the Bristol Conference.

An anion-vacancy occupied by an electron (F-center) and other combinations of vacancies and other imperfections will be discussed in the next paragraph.

### C. Foreign atoms

A nonmagnetic foreign atom, either in a regular or interstitial site, will have a negligible effect on the magnetic field produced at the position of surrounding nuclei.

Magnetic impurities will produce a large local field, of the order of  $10^3$  oersted, at nuclei which are nearest neighbors, but this field will drop off as the inverse cube of the distance. Consequently the resonance absorption of nuclei in the immediate neighborhood will be displaced and contribute to the far wings of the absorption line, which in general will remain unobserved. The bulk of the nuclei will be practically unaffected and the second moment of the observed signal will remain almost the same.

Furthermore, the magnetic field of the impurity is not static but changes with the spin orientation of the magnetic ion. The characteristic time is the electron spin lattice relaxation time of the impurity. For paramagnetic salts with high concentrations of magnetic ions the characteristic time could alternatively be determined by the spin-spin or exchange interaction, whichever is the fastest. For isolated magnetic imperfections the spin-orbit lattice coupling is the only mechanism causing variation of spin orientation with time. It has been shown conclusively [2,7,8] that in many ionic and valence crystals the nuclear spin lattice relaxation time is determined by the presence of these magnetic imperfections. They can be chemical impurities of the transition group elements, F-centers, filled donor or acceptor levels in semiconductors, or other imperfections provided they are carriers of electronic magnetism.

The nuclear spin relaxation takes place by the following sequence of events [7]. An absorbed quantum  $h\nu_0$  is transported by spin diffusion through the nuclear spin system toward the neighborhood of a paramagnetic impurity. This process is independent of the lattice temperature. The quantum  $h\nu_0$  is then transferred to the lattice. The lattice vibrations modulate the orbit of the magnetic imperfections and via the spin orbit coupling flip the electronic spin. The time-dependent local field of this electron spin in turn flips the nuclear spin. This process is determined by the electron spin lattice relaxation time, which depends on the lattice temperature. In principle the measurement of the nuclear relaxation time as a function of temperature will give information about the concentration of paramagnetic imperfections and their spin lattice coupling. It should be pointed out that much more detailed information is obtained from the observation of the electron spin resonance of the impurity itself. The significance in the case of nuclear resonance is

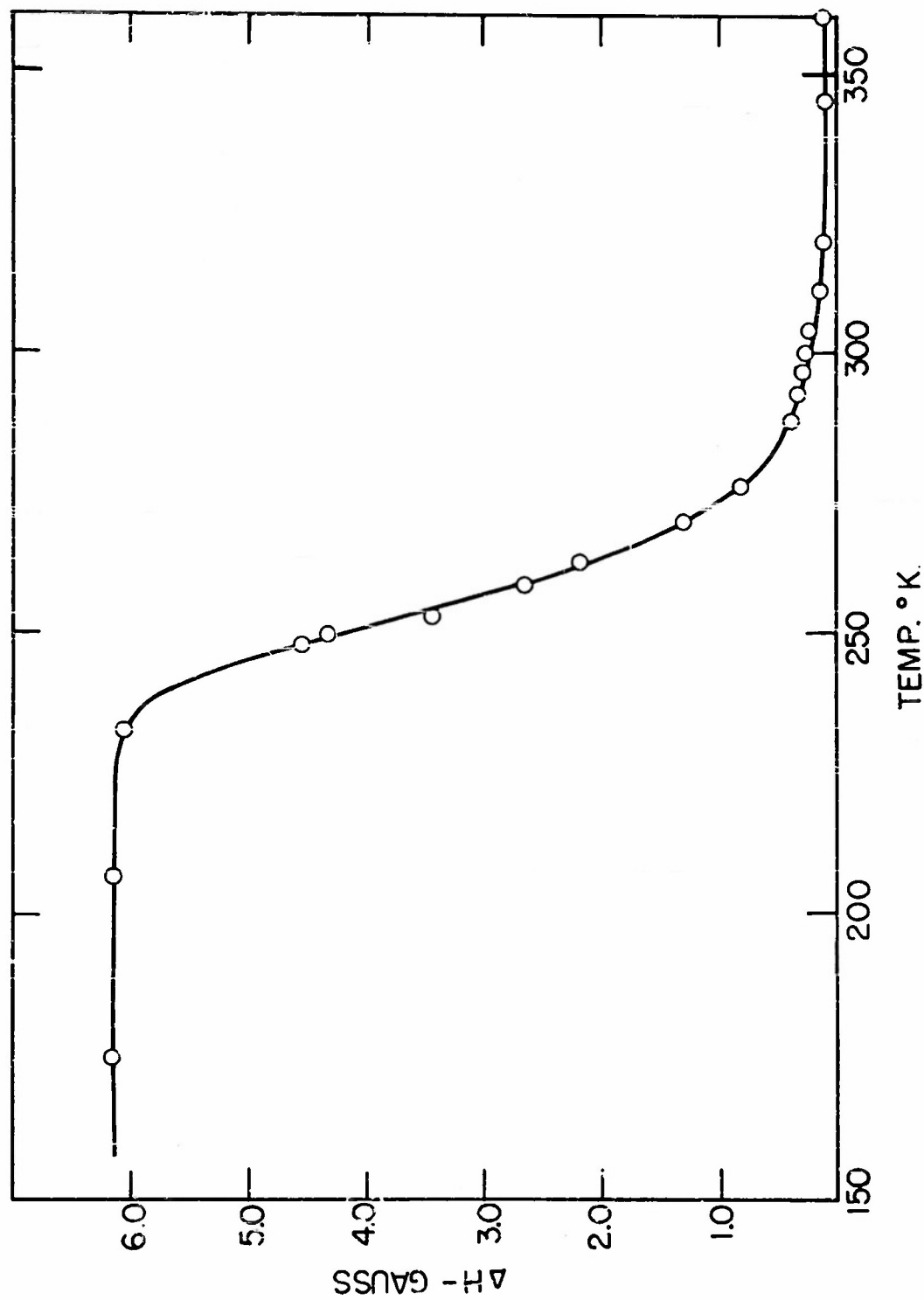


Fig. 1. The line width  $\Delta H$ , measured between points of maximum slope, of the  $\text{Li}^7$  resonance absorption in metallic lithium as a function of temperature. From the diffusional narrowing the activation energy for the self-diffusion of  $\text{Li}^7$  is determined as 9.8 kcal/mole. (Gutowski and McGarvey).

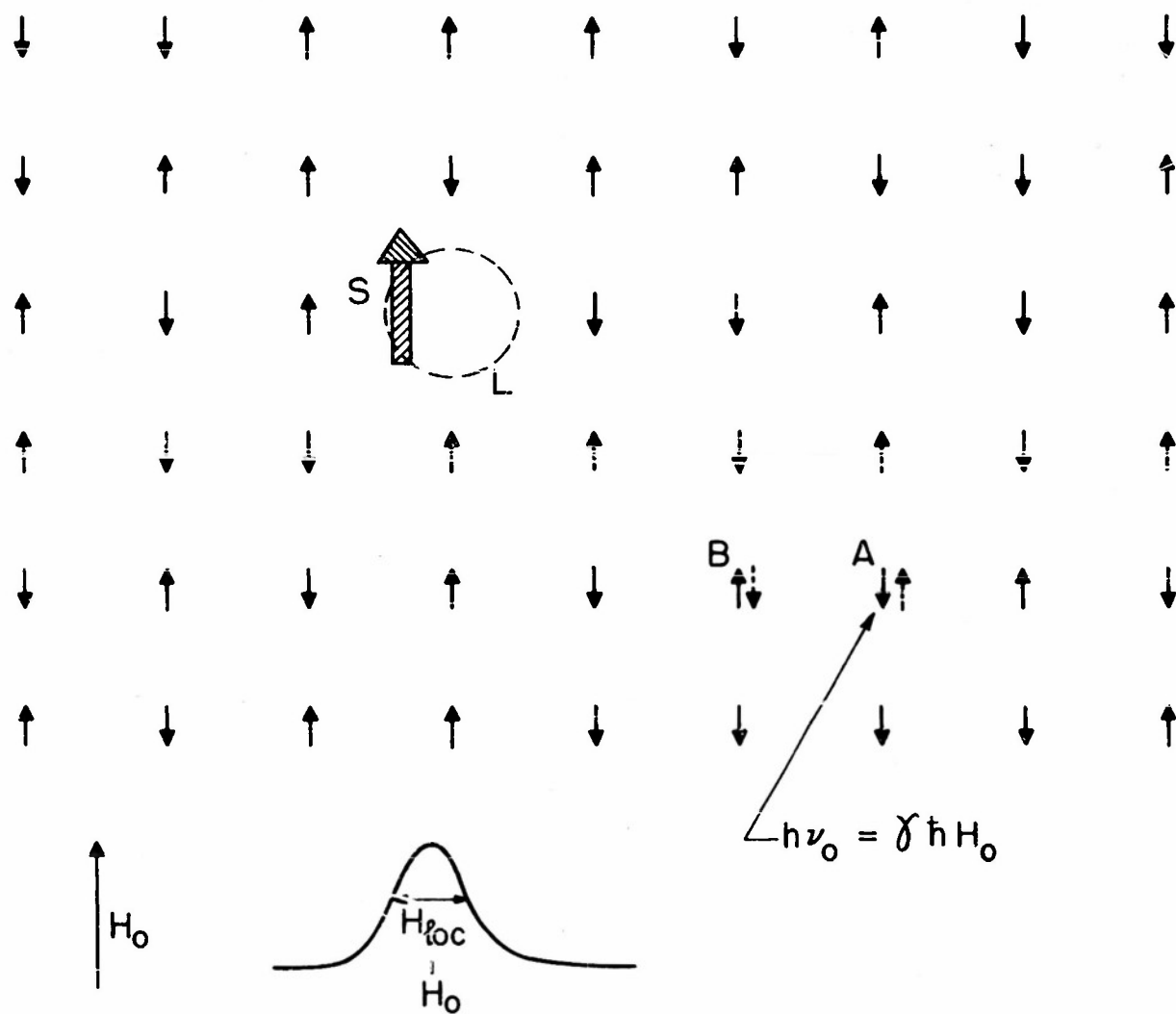


Fig. 2. A lattice of nuclear spins with a paramagnetic impurity. The resonance is spread out over the range of local fields produced by neighboring dipoles. A quantum  $h\nu_0$ , absorbed by spin A, is transferred to the site B by a simultaneous spin flip. The magnetic energy quantum diffuses toward the impurity. It is transferred to the lattice via interaction with the electron spin S and the spin-orbit coupling.

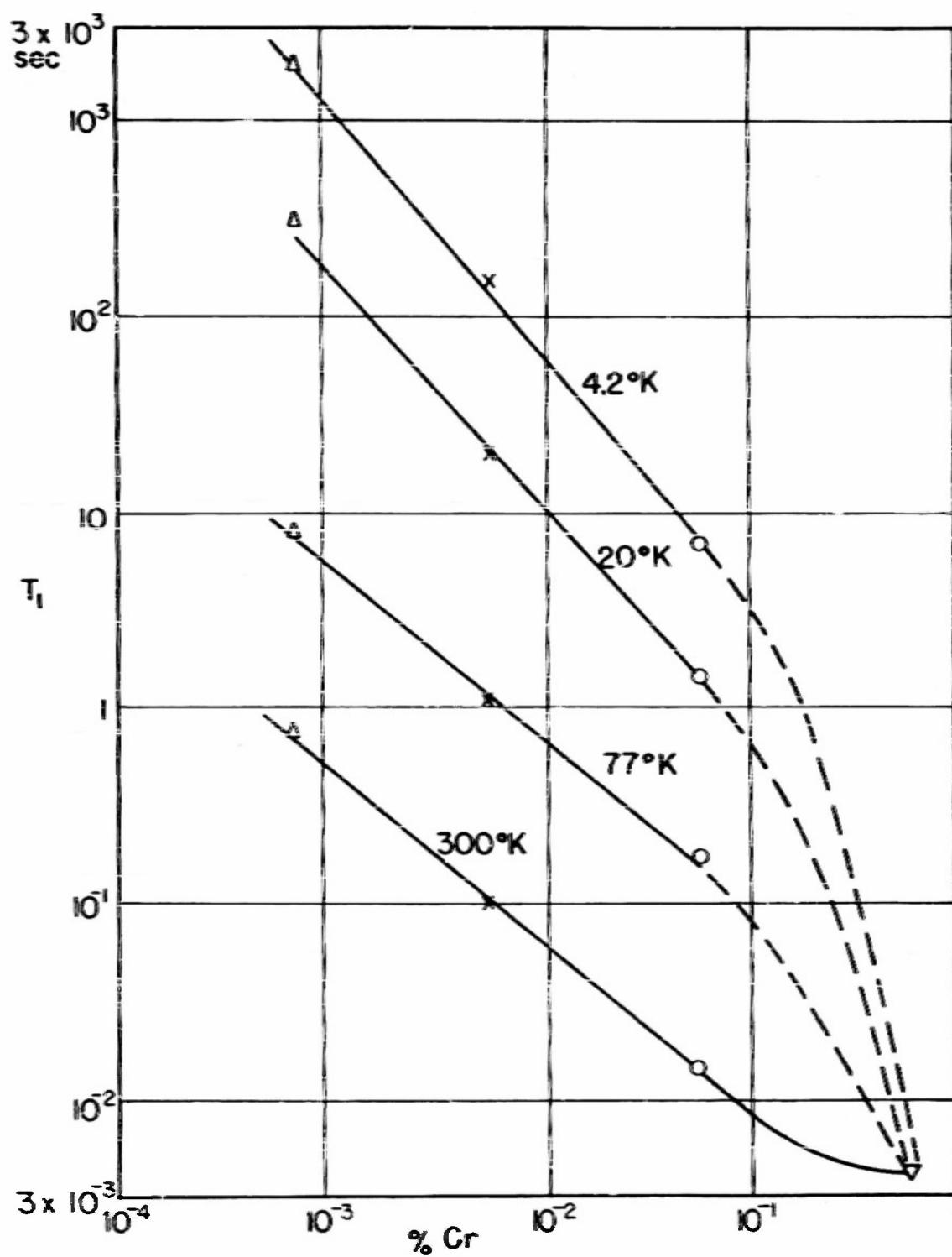


Fig. 3. The nuclear relaxation time  $T_1$  of protons at 30.5 Mc/s in  $\text{KAl}(\text{SO}_4)_2 \cdot 12\text{H}_2\text{O}$  with controlled  $\text{Cr}^{+++}$  impurities (% weight).

mainly that these impurities provide an adequate relaxation mechanism.

#### D. Electrons and holes

Since free electrons and holes are carriers of an electronic spin, they create internal magnetic fields which interact with the nuclear spins. It is a matter of taste whether one wishes to consider the conduction electrons in a metal as imperfections, but in semiconductors this is certainly the generally accepted point of view. To achieve a uniform presentation conduction electrons will be considered as imperfections in this paper.

In a metal with Fermi energy  $E_F$  most of the electron spins are paired off and only a fraction of the order of  $\beta H_0/E_F$  has unbalanced magnetic moments. The Pauli paramagnetism of the conduction electrons gives rise to a shift of the nuclear resonance in metals to higher frequencies, first discovered by Knight [9]. The relative shift is given by [10,11]

$$\frac{\Delta H}{H_0} = \frac{\Delta \omega_{is}}{\nu_0} = \frac{\beta A}{h} \frac{\langle |\psi_{\text{met}}(0)|^2 \rangle_{Av}}{|\psi_{at}(0)|^2} v_a N(E_F) \quad (6)$$

where  $\beta$  is the Bohr magneton,  $A \cdot S$  is the hyperfine interaction in the corresponding atomic state;  $\langle |\psi_{\text{met}}(0)|^2 \rangle_{Av}$  is the square of the electronic wave function in the metal evaluated at the position of the nucleus, normalized over the atomic volume  $v_a$  and averaged over the Fermi surface.  $N(E_F)$  is the density of states of the conduction electrons at the Fermi surface, per unit volume and per unit energy interval. The observed relative shifts range from 0.0261 per cent for  $\text{Li}^7$  to 2.5 per cent for  $\text{Hg}^{199}$ . There is a general increase with increasing atomic number, as the hyperfine interaction becomes larger.

In alloys the shift given by equation (6) may vary [11] and will indicate a variation in the product of the density of states, the atomic volume and the probability density of the electrons at the nucleus. In fact, the product may show a dispersion and have different values at different nuclei depending on the relative position of the impurities in the neighborhood. In general this will give rise to a spurious asymmetric broadening of the line.

Mott [12] and Friedel [13] have calculated the shielding of the extra charge on the Zn atom by the concentration of conduction electrons around

it. The shielding is practically complete already at the nearest neighbors and since the impurity was introduced as a neutral atom, the electron density throughout the bulk of the metal is unchanged.

However, the Knight shift is not determined by the total density of conduction electrons but by  $|\psi_k(0)|^2$  evaluated at the Fermi surface. One-electron wave functions with a fixed magnitude of the wave number  $k$  must be evaluated in the neighborhood of the impurity. Brooks \* has pointed out that in the same free electron approximation as used by Mott the square of the wave function for electrons with a given value of  $k$  falls off more slowly than the exponential law. The value  $k$  corresponding to the momentum at the Fermi level must be taken. Mott's result of exponential shielding is obtained by integration over all occupied values of  $k$ . Reliable values for the shift can only be obtained if the wave equation in the periodic crystalline potential, perturbed by the impurity, is solved. It is clear that  $|\psi_{\text{met}}(0)|^2$  will be a function of  $r$ , the distance from the impurity. It may show some oscillations before leveling off to its value in the bulk of the metal.

For very low impurity concentrations the main absorption peak should remain undisplaced with some small (usually unobservable) contributions on either side from nuclei near the impurity. For concentrations larger than a few per cent, a broadening of the line is caused by the distribution of shifts, and the frequency of maximum absorption may change since the majority of the nuclei are now near an impurity. These effects have been observed qualitatively for solutions of tin in thallium, as shown in Fig. 4. There is, however, some uncertainty about the phase diagram and a two-phase region may exist between 4 and 10 per cent atomic per cent tin. Furthermore, the line broadening was not asymmetric as might in general be expected. If the increase in width is indeed due to a dispersion of Knight shifts, and therefore proportional to  $v_0$ , the increase will be more pronounced in high fields. More precise measurements on various alloy systems with spin  $I = 1/2$  are badly needed.

It is a matter of taste whether one wishes to consider the alloys with a high concentration of solute atoms as imperfect crystals. As there is no clear-

-----  
\*Private communication.

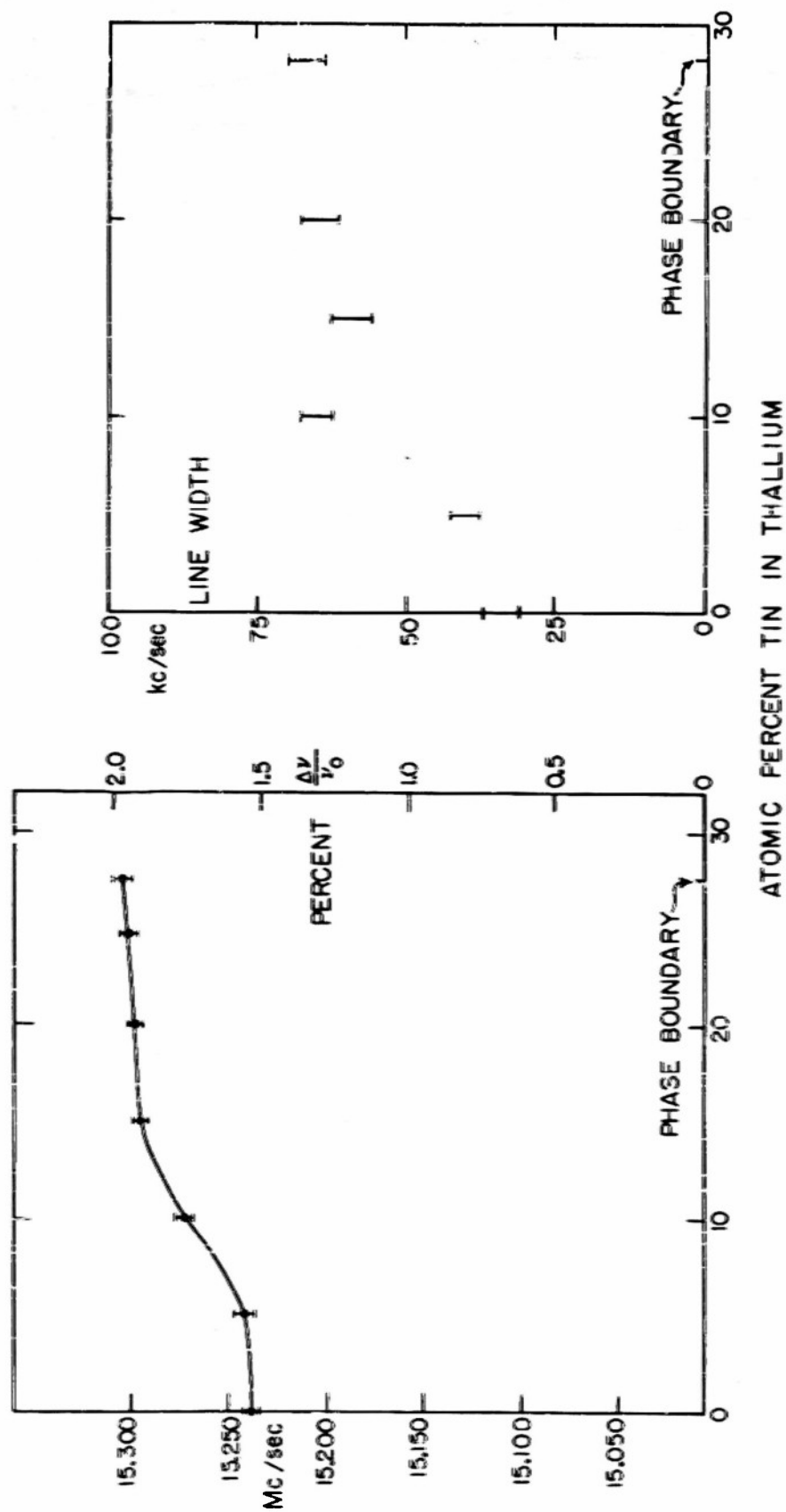


Fig. 4. a) The frequency of maximum absorption, b) the line width between points of maximum slope of the  $Tl^{205}$  resonance in thallium-tin alloys.

cut concentration at which an impurity becomes a regular component of the solid, alloys will be considered as imperfect solids in this review to allow for a convenient general presentation of the subject.

Whereas the Knight shift changes continuously with composition in a solid solution, discontinuous changes are expected in going from one phase to another. In two-phase regions the nuclear resonance is doubled. This has been observed for the  $Tl^{205}$  resonance in the thallium-mercury system [11].

In the liquid phase, and perhaps also just below the melting point, the nuclei will diffuse rapidly and the resonance frequency will be determined by the average value of the product  $v_a |\psi_{met}(0)|^2 N(E_F)$ , where the average is taken over all configurations around the nucleus in question. Instead of the dispersion of Knight shifts, the center of gravity is measured in the liquid. An asymmetric impurity broadening in the solid corresponds to a variation of the resonance frequency in liquid. This last effect is, in terms of Seitz's classification, the combined influence of three types of imperfections: electrons, foreign atoms and vacancies.

The shift caused by conduction electrons in semiconductors is negligible [14]. The total density of electrons and also of those with unbalanced spin is so much smaller than in metals that no observable effect results.

The nuclear relaxation in metals is usually also determined by the interaction of nuclear spins and conduction electron spins. A simple picture is that the nuclear spin has a certain probability to make a transition, whenever an electron in the electron gas passes by. Only a small fraction of the electrons, of the order of  $kT/E_F$ , representing the tail of the Fermi distribution, are allowed to take up the small energy differences involved in the magnetic transition. The relaxation time should be independent of the external field  $H_0$ , although experimentally some variations of  $T_1$  with  $H_0$  have been observed. If one takes into account only the point-interaction caused by the finite value of the wave function at the position of the nucleus the following relation due to Korringa [15] exists between the relaxation time and the shift.

$$T_1 \left( \frac{\Delta\nu_{is}}{\nu_0} \right)^2 = \frac{h}{\pi kT} \left( \frac{\beta}{\gamma \hbar} \right)^2 \quad (7)$$

The relaxation time gives the product of the same quantities  $v_a |\psi_{inc}(0)|^2 N(E_F)$  as the shift.

Actually the part of the electronic wave function with non S-character (p-, d-, etc.) will also contribute to the relaxation time, but not to the shift. The equal sign in equation (7) should therefore be replaced by a  $\leq$  sign. This correction of the Korringa relation is probably more important than the neglect of correlation and exchange effects in the electron-gas model. The observed deviations from the Korringa relation, which are mostly in the right direction [16], could perhaps find an explanation in this fashion.

Although the hyperfine interaction of p- and d-orbits is usually much smaller than in S-states, the amount of S-character of the one-electron wave functions may be small even in alkali metals. Jones and Schiff [17] estimate that in sodium there is 60 per cent S-character and in lithium 25 per cent. Assuming the hyperfine interaction in the p-state to be only 10 per cent of that in the S-state, the interaction of the p-part would reduce the relaxation time calculated from the Korringa relation by 40 per cent in lithium. A careful systematic check of this relation is desirable.

The relaxation time in semiconductors will usually be determined by electron spins. It is predicted that the spins of bound electrons or holes which act like paramagnetic impurity atoms will produce a more efficient relaxation mechanism, discussed in the preceding paragraph, than the spins of free carriers [14]. No experimental evidence is available, but in principle the nuclear relaxation could give a completely independent determination of the number of bound electrons or free carriers in semiconductors.

In noncubic crystals the p-, d- etc. character of the electron orbitals gives rise to an anisotropy of the Knight shift, which has been observed [11] in white tin and solid mercury. Figure 6 illustrates how an ellipsoidal distribution in space of the density of electrons with unbalanced spins will give rise to an aiding or counteracting local field on the nucleus, depending on the direction of  $H_0$  with respect to the crystallographic axes (= axes of the electron density). In polycrystalline samples, which must necessarily be used in resonance work on conductors, the line gets a characteristic asymmetric shape. The observed anisotropy is proportional to the field strength, as it increases proportionally to the number of electrons with unbalanced spin in

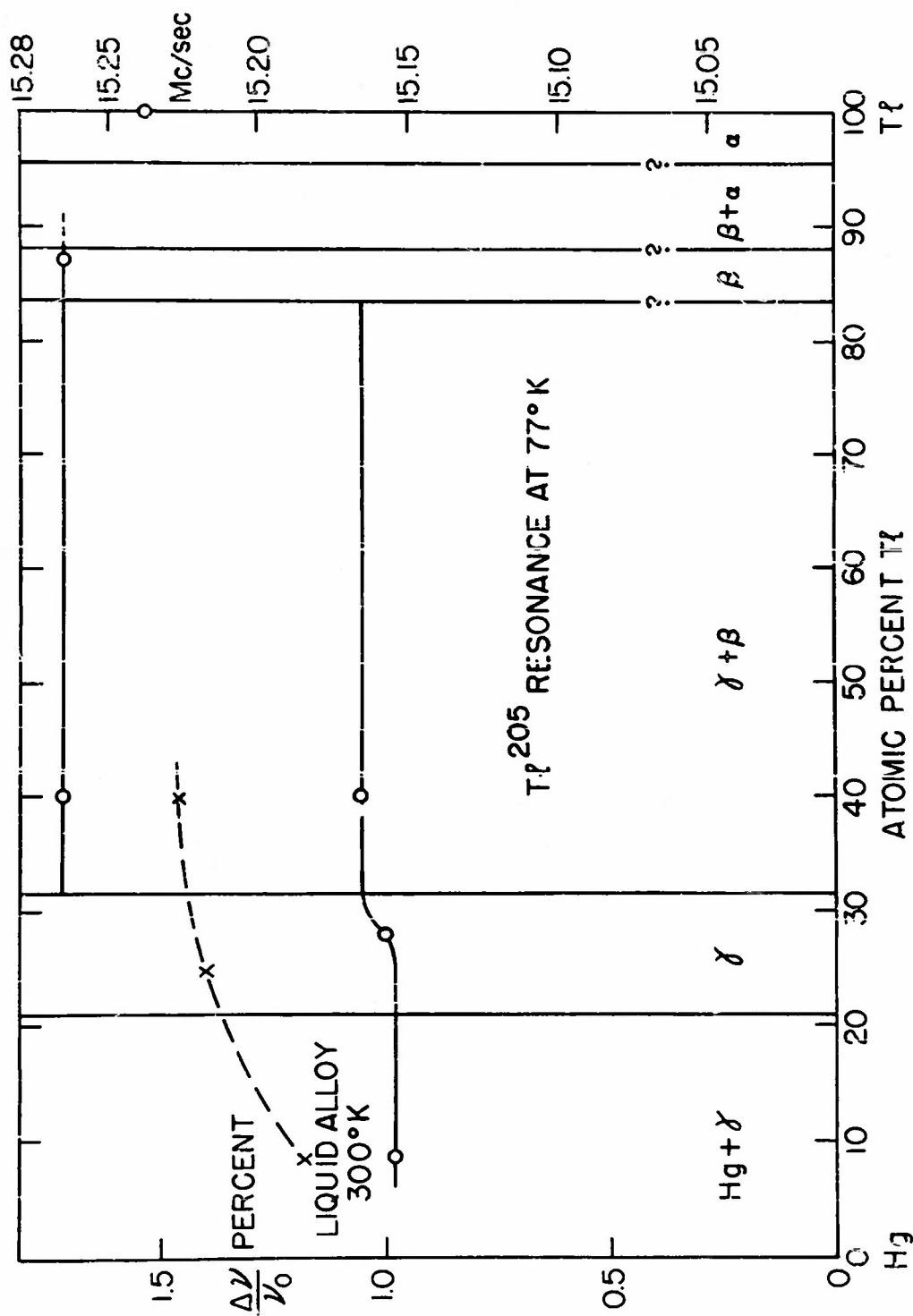


Fig. 5. The  $Tl^{205}$  resonance frequency in the Tl-Hg system. The Knight shift varies continuously with composition in each phase, and changes discontinuously from one solid phase to another. The indicated phase boundaries do not apply to the liquid phase. In two-phase regions two resonance lines occur. In the  $\alpha + \beta$  region an unresolved structure was observed which is not indicated in the figure.

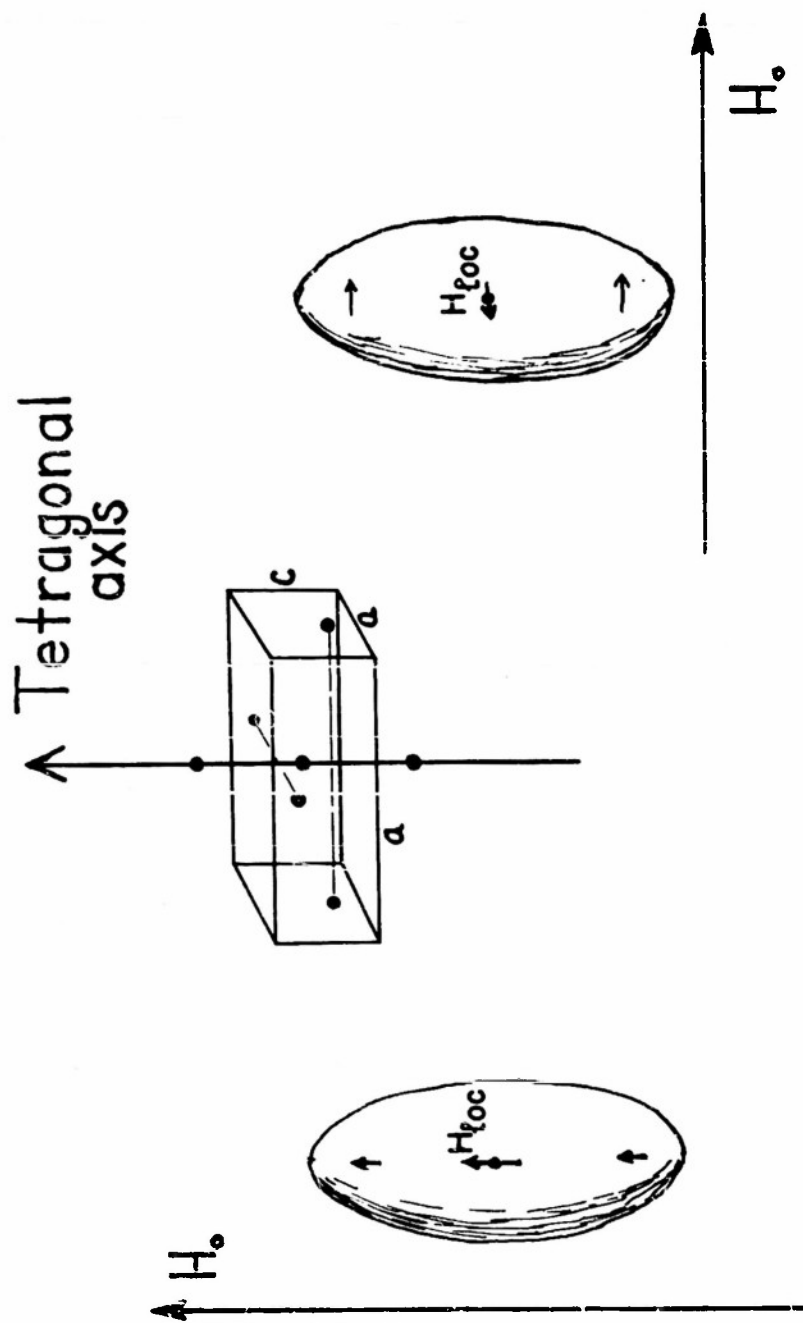


Fig. 6. The anisotropic distribution of the conduction electrons with unbalanced spin in  $\beta$ -tin around a tin nucleus. This causes an anisotropy of Knight shift in noncubic metals.

the same manner as the isotropic shift.

$$\frac{\Delta\nu_{||} - \Delta\nu_{\perp}}{\nu_0} = 3\beta^2 v_a N(E_F) q_F + \frac{g_{||} - g_{\perp}}{g_{av}} \Delta\nu_{is} \quad (8)$$

The first term arises from the deviation from cubic symmetry

$$q_F = \int \psi_F r^{-5} (3z^2 - r^2) \psi_F^* dV$$

of the density of electrons near the Fermi level. The second term is caused by the anisotropy in the g-factor of the conduction electrons. Unfortunately we have only one relation between  $q_F$  and  $g_{||} - g_{\perp}$ . Both quantities are difficult to determine theoretically and experimentally by other means. If the anisotropy is small, the effects can be made observable in very high fields  $H_0$ .

In alloys one will have, in addition to the distribution of isotropic shifts, a distribution of anisotropic shifts. This will add to the broadening of the resonance in such systems.

Although there is no experimental evidence, we wish to point out the possibility of investigating order-disorder transitions in alloys in this manner. In the first place there will be an obvious change in the dipolar contribution to the line width on ordering, which can be calculated with equation (1). This change in width will be especially marked if the other constituent in the binary alloy has zero spin. In the second place the dispersion in the Knight shift will cease to exist in the completely ordered state. Ordering will in general be accompanied by a marked change in the line width.

Since the width of the nuclear resonance is largely determined by the near neighbors, it is a good indicator for short-range order without the complications of temperature diffuse scattering which are inherent in the X-ray technique.

The onset of precipitation will also cause a change in composition of the immediate environment. The precipitation hardening in a system with solvent atoms with  $I=0$  and solute atoms with  $I=1/2$  may be studied profitably. The nuclear resonance will broaden, when a phase rich in solute atoms precipitates.

### E. Phonons

Lattice vibrations will modulate the dipolar interaction between nuclear spins and thus produce a relaxation mechanism. In fact, this was historically the first magnetic spin lattice relaxation mechanism, proposed by Waller [17] in 1932 for electron spin systems. It can be shown that nuclear relaxation times calculated by this theory are in general a factor of  $10^3$  to  $10^6$  longer than observed. The dominant relaxation mechanism in metals is caused by conduction electrons; in ionic and valence crystals frequently by paramagnetic imperfections. The energy in the former case is taken up by a change in momentum of the electrons; in the latter case the lattice vibrations are essential to the transfer of energy. The relaxation is thus strictly speaking a combined effect of two imperfections.

In many molecular and certain other crystals different types of thermal motion than lattice vibrations occur, such as hindered rotation tunneling between two or more positions of equilibrium. Such motions, which produce a very effective relaxation mechanism for nuclear spins, should perhaps also be considered as imperfections of the perfect rigid lattice. A wealth of experimental data exists on this matter, for which the reader is referred to the literature [18]. In this context the diffusion phenomena discussed under (b) should be considered as the combined effect of vacancies and phonons.

### F. Excitons

An excited atom or ion in a solid will have no effect, if the excited state is nonmagnetic. If the state is magnetic, it will have a similar effect on nuclear relaxation as a paramagnetic impurity. The characteristic time of its local field will be determined by the life time of the excited state, by its diffusion through the lattice or by its spin reversal time, whichever process is the fastest. No experimental evidence is known to the author. The concentration of excitons is usually too low, but a change in nuclear relaxation time in phosphors under strong illumination might be detectable.

## III

### Quadrupole Effects

If the nuclear spin  $I \geq 1$ , the interaction of the imperfection with the

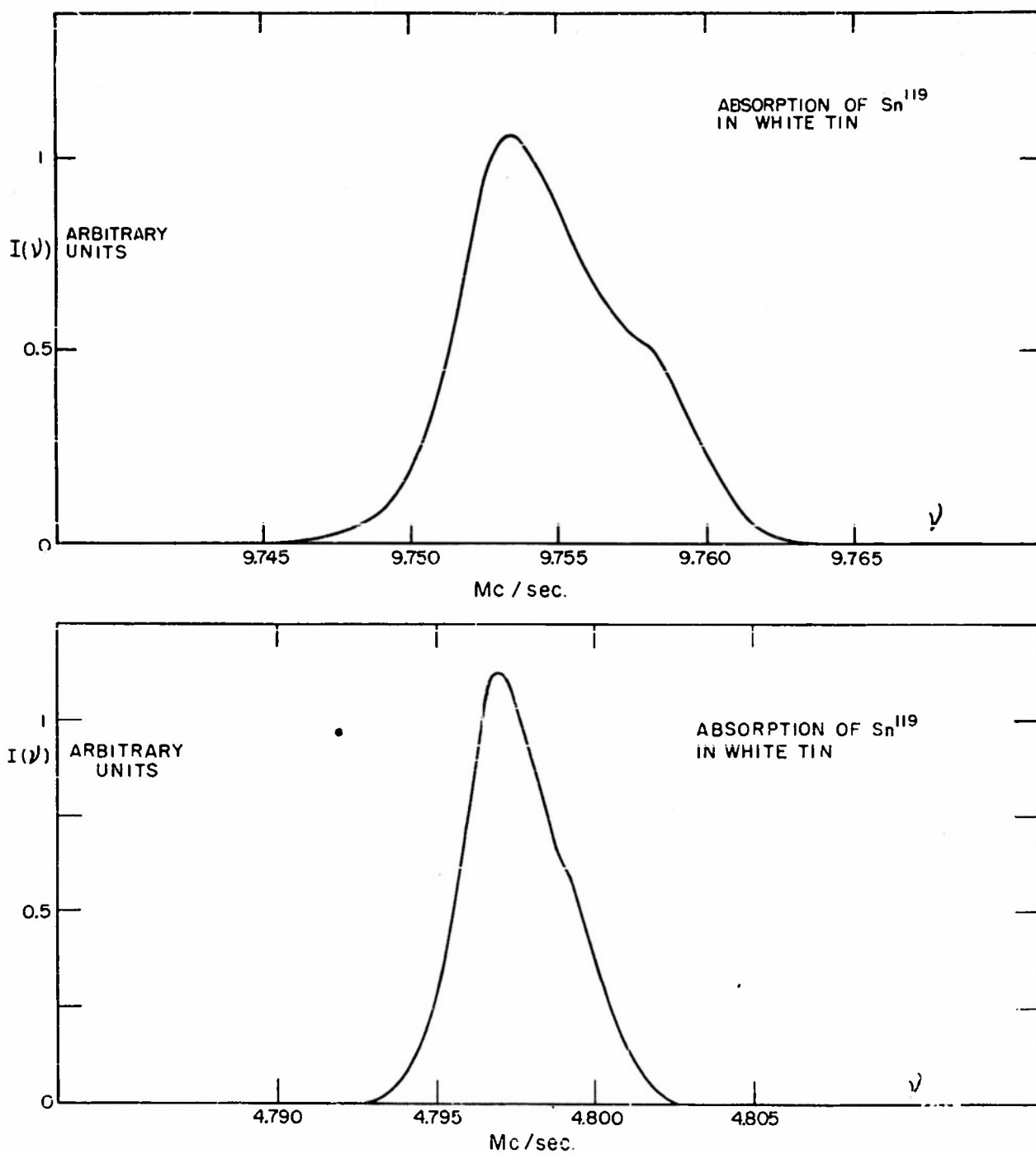


Fig. 7. The observed asymmetric nuclear resonance in polycrystalline  $\beta$ -tin. The anisotropy in the Knight shift is proportional to the resonant frequency. The asymmetry is more pronounced in the recorded derivatives.

electric quadrupole moment will frequently be more important. The crystalline electric field will always be disturbed by the imperfection, and special magnetic properties of unbalanced electron spins are not required.

The elements of quadrupole interaction in an inhomogeneous electric field of axial symmetry will first be recalled [19, 20]. Assume that the quadrupole interaction can be considered as a small perturbation on the  $2I + 1$  equally spaced energy levels in the magnetic field  $H_0$ , which is taken in the  $z$ -direction. The equal spacing will be destroyed. Introduce a scalar quantity

$$eq = \sum_j e_j (3 \cos^2 \phi_j - 1) r_j^{-3}$$

where  $\phi_j$  is the angle between the radius vector  $r_j$  toward a charge  $e_j$  in the lattice and the axis of symmetry at the origin. Denote the angle between this symmetry axis and the magnetic field by  $\theta$ . Then the energy difference between the levels  $m_I$  and  $m_I - 1$  of the nuclear spin is given by first-order perturbation theory.

$$\Delta E_{m \rightarrow m-1} = h \nu_0 + (2m-1)(3 \cos^2 \theta - 1) \frac{3e^2 q Q}{8I(2I-1)} \quad (9)$$

where  $Q$  is the nuclear quadrupole moment. It is seen from equation (9) that the distance between the levels  $m_I = 1/2$  and  $-1/2$  is unperturbed in this approximation. Second-order perturbation theory gives for the energy difference between these levels if the nuclear spin is an odd half-integer,

$$\Delta E_{1/2 \rightarrow -1/2} = h \nu_0 + \frac{9}{64} \frac{2I+3}{4I^2(2I-1)} \frac{e^4 Q^2 q^2}{h^2 \nu_0^2} (1 - 9 \cos^2 \theta)(1 - \cos^2 \theta) \quad (10)$$

The splitting of the nuclear resonance has been observed by Pound [19] and others [20] in noncubic single crystals. In cubic crystals, or, more accurately, at points around which the symmetry is cubic,  $q = 0$  and there is no quadrupolar interaction. In polycrystalline noncubic crystals the resonance of the satellite lines, i. e., the transitions excluding the central component  $m_I = 1/2 \rightarrow -1/2$ , will be spread over a large frequency interval, as  $3 \cos^2 \theta - 1$  ranges from its maximum value of 2 to its minimum value of -1. An inte-

gration over the solid angle  $\sin\theta d\theta d\psi$  yields for the absorption in a powdered sample the line shape [21] shown in Fig. 9. In second approximation even the central component will be broadened and its asymmetric shape for a polycrystalline sample is given in Fig. 10. On these curves the dipolar broadening ought to be superimposed. A similar curve had been given by Nierenberg and Ramsey [22] in molecular beam experiments on alkali-halide molecules. The observation technique of nuclear magnetic resonance makes it very difficult to detect the broad low tails of these patterns. With the usual modulation method the slope of the absorption curve is detected and this quantity varies inversely as the square of broadening.\* Frequently only the absorption near the resonance peak can be observed. The quantity  $g(\nu_{\max})$  will decrease as the quadrupole interaction increases, the total area under the absorption curve remaining constant. It will be useful to introduce normalized shape functions for each satellite and for the central component separately. For the complete line we have

$$g(\nu) = 0.4 g_c(\nu) + 0.6 g_s(\nu) \text{ for } I = \frac{3}{2} \quad (11)$$

and

$$g(\nu) = \frac{9}{35} g_c(\nu) + \frac{8}{35} g_{3/2,1/2}(\nu) + \frac{5}{35} g_{5/2,3/2}(\nu) \\ + \frac{8}{35} g_{-1/2,-3/2}(\nu) + \frac{5}{35} g_{-3/2,5/2}(\nu) \\ \text{for } I = 5/2, \text{ etc.}$$

In crystals with noncubic symmetry a splitting of the nuclear spin levels occurs even in the absence of a magnetic field, as indicated in Fig. 8. Transitions between these levels give rise to so-called pure quadrupole resonance lines [23], although it should be remembered that the transitions are always induced by a magnetic radiofrequency field. A single crystal is not needed, as the magnetic field is absent. In powders the lines will broaden immediately upon application of an external field. We shall now discuss the influence of the various imperfections.

\* When a square-wave modulation, on- and off-resonance, is used, the signal is inversely proportional to the broadening itself.

# SPIN $I = \frac{3}{2}$ IN AXIAL ELECTRIC FIELD

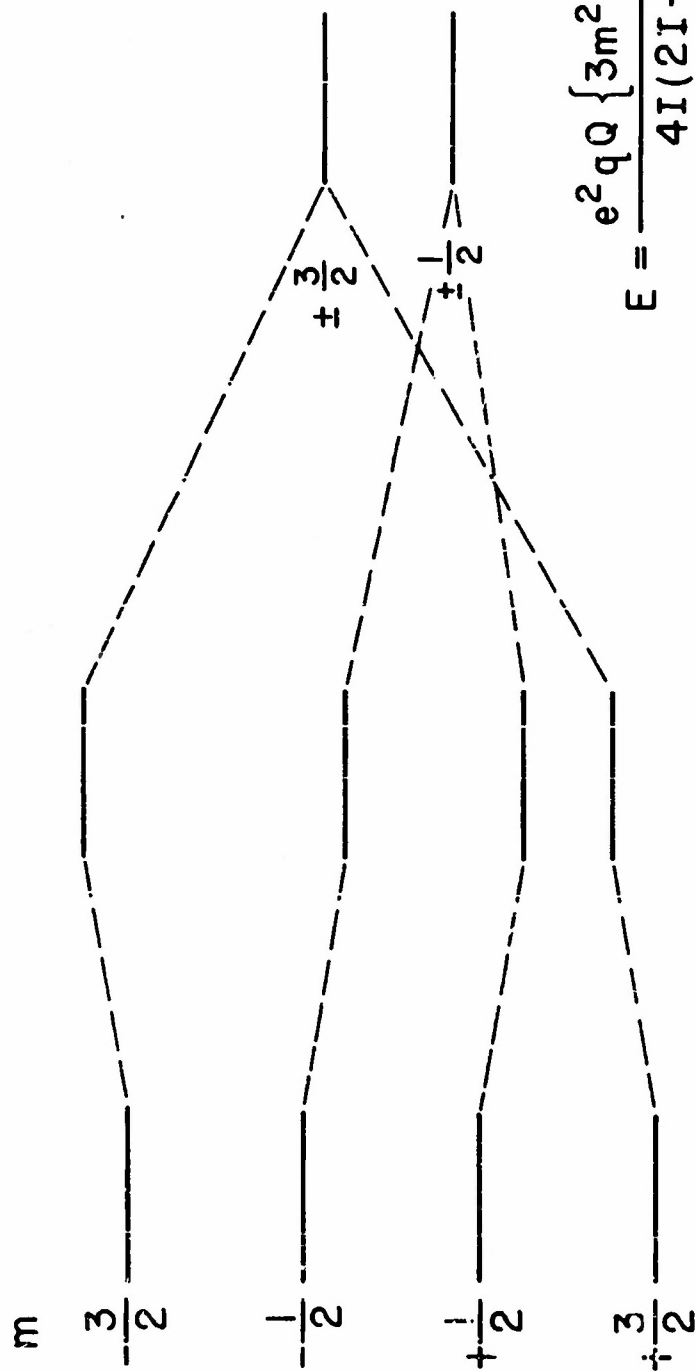


Fig. 8. Energy levels of a nuclear spin with  $I = 3/2$  in a magnetic field with cubic environment, first-order perturbation in an axially symmetric field and the zero magnetic field splitting.

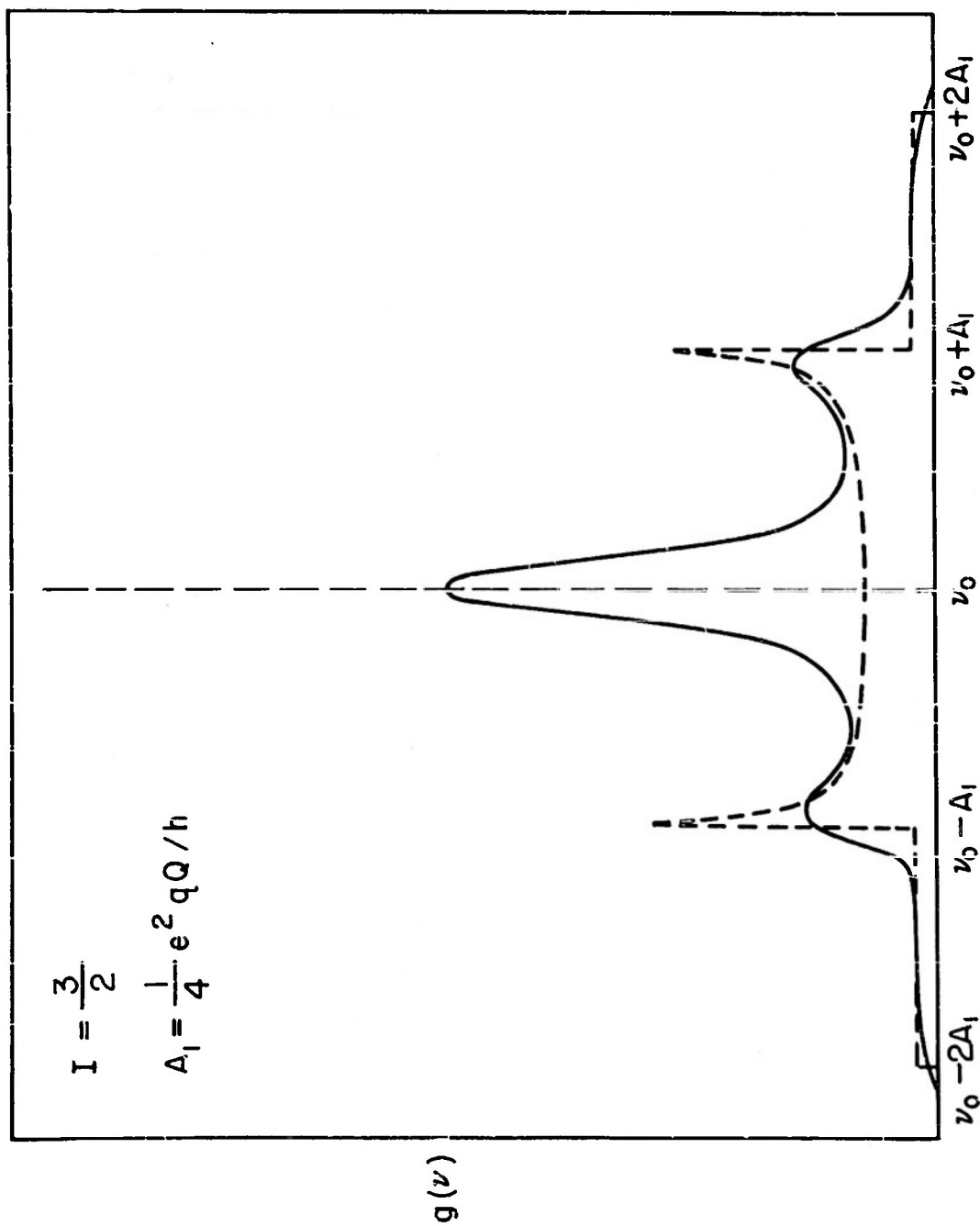


Fig. 9. First-order quadrupole perturbation. Line shape for  $I = 3/2$  in powdered samples of axially symmetric crystals (dashed line). With dipolar broadening superimposed the drawn curve results. Frequently the satellites are spread out over such a large frequency range that the wings become unobservable.

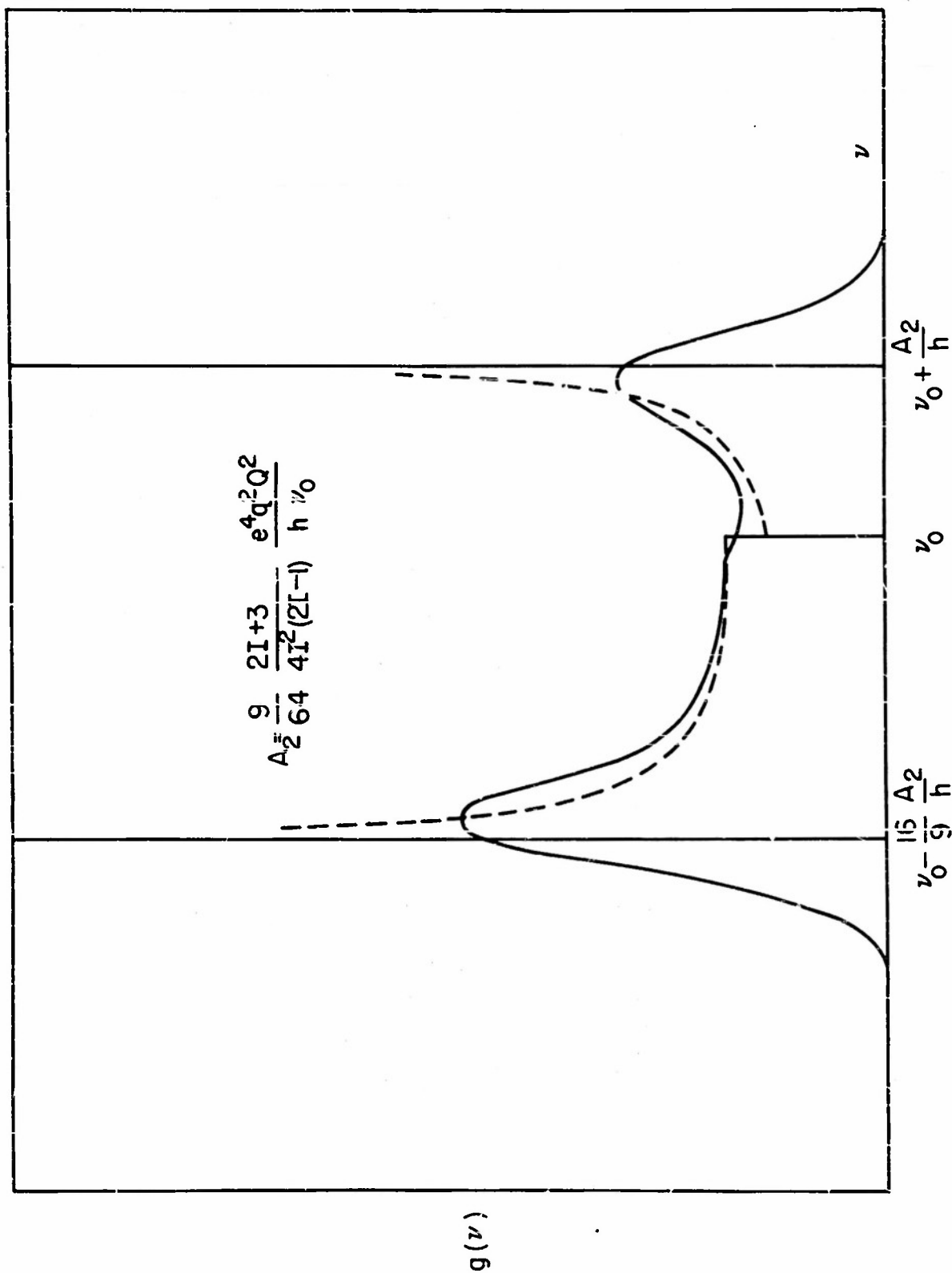


Fig. 10. Line shape of the central component ( $m_I = \frac{1}{2} \rightarrow -\frac{1}{2}$ ) in powdered samples of axially symmetric crystals. The transition is asymmetrically broadened by second-order quadrupole interaction (dotted line). The superposition of the dipolar interaction gives the drawn curve (comp. Nierenberg and Ramsey).

### A. Dislocations

The strain field around a dislocation line will produce a change in the gradient of the electric field at the nuclei near the dislocation. The change in gradient  $\Delta q$  will be proportional to the strain, which in turn is inversely proportional to the distance from the dislocation line. A distribution of gradients  $q$  and of angles  $\theta$  will be created. Actually the nuclei will be at points where the axial symmetry is lost. Formulae for the quadrupole interaction in fields of lower symmetry have been worked out [20]. Qualitatively the results for a distribution of gradients with or without axial symmetry will be the same. A general broadening of the components of the resonance will occur. The central component will only be affected in second-order approximation. In noncubic single crystals dislocations will broaden the satellites much more than the central component. The latter, which is of course only present if the nuclear spin is an odd multiple of one half, is broadened inversely proportional to the magnetic field  $H_0$ .

The strains will distort the cubic symmetry in cubic crystals. Before the deformation all components coincide in the single crystal or polycrystalline sample of cubic symmetry. After the deformation the satellite components will be broadened so much that they are frequently unobservable, and only the central component remains. Watkins [24] discovered this effect for the bromine and iodine resonances in rather perfect crystals of KBr and KI. He introduced a calibrator into the experimental apparatus which made (absolute) intensity measurements possible. The intensity of these resonances corresponds to that of the central component alone, namely 0.4 of the total intensity for the bromine isotopes with spin  $I = \frac{3}{2}$ , and  $\frac{9}{35}$  for iodine with  $I = \frac{5}{2}$ . When the crystals were subjected to severe cold work (plastic flow resulting in a 22 per cent change in dimension along the 100 axis) the asymmetric broadening of the central component was also observed. Superimposed on the plastic deformation effect was a reversible broadening of 3 per cent to elastic strains. The order of magnitude of the quadrupole interaction in the stress field of these dislocations may be obtained from the following, admittedly very crude, argument.

Consider first the change in electric field gradient, if a neighboring charge  $e$  at distance  $r$  is displaced over a distance  $\Delta r$ . One finds for the

the change in gradient due to this compressional strain  $\epsilon = -\Delta r/r$

$$\Delta(\text{eq}) = 6e r^{-3} \epsilon$$

The actual gradient at the nucleus is not produced by the displacements of bare charges. The gradient at the nucleus is a very sensitive function of the distortion of the ion core around it. Relatively slight distortions of this core can produce large distortions in the symmetry of the wave function in the immediate neighborhood of the nucleus. Since the electron density is weighted by a factor  $r^{-3}$  in the nuclear quadrupole interaction, the actual gradient at the nucleus may be increased by an antishielding factor  $1 + |\gamma_{\infty}|$  which has been calculated by Foley and Sternheimer [25] for a number of ions. They find that this factor  $1 + |\gamma_{\infty}|$  is 47.5 for  $\text{Cl}^-$ , 9.7 for  $\text{Cu}^+$ , 51.2 for  $\text{Rb}^+$  and 98.8 for  $\text{Cs}^+$ . The order of magnitude of the quadrupole interaction is changed by this factor.

The ion core around a given nucleus can be distorted not only by the displacement of external charges, but also by the interaction with neighboring ion cores. In general there will be an interplay between the charge or "valance" effect and the "size" effect of the ion cores. Both effects will presumably be important in the case of crystal deformation. A generalized multiplication factor  $\lambda$  is introduced for each crystal lattice, which takes account of the ion core distortion in the strained lattice, and we write for the change in quadrupole interaction

$$\Delta(\text{eq}) = 6\lambda e a^{-4} \Delta a = 6\lambda e a^{-3} \epsilon$$

where  $a$  is the distance between nearest neighbors and  $\epsilon$  is a measure of the strain. The effect of all neighbors is incorporated in  $\lambda$ , which is a dimensionless constant (more precisely a fourth-order tensor) in the assumed proportionality between the strain and the change in gradient at the nucleus. For a cubic lattice under hydrostatic pressure the net effect would of course be zero, but at a distance  $r$  from a dislocation line with Burger's vector  $b$  we may estimate the order of magnitude of  $\epsilon$  as  $br^{-1}$ . The stress field around the dislocation line drops off inversely proportional to the distance [26]. As  $b$  is of the same magnitude as  $a$ , we obtain

$$\Delta(\text{eq}) = 6\lambda e a^{-2} r^{-1}$$

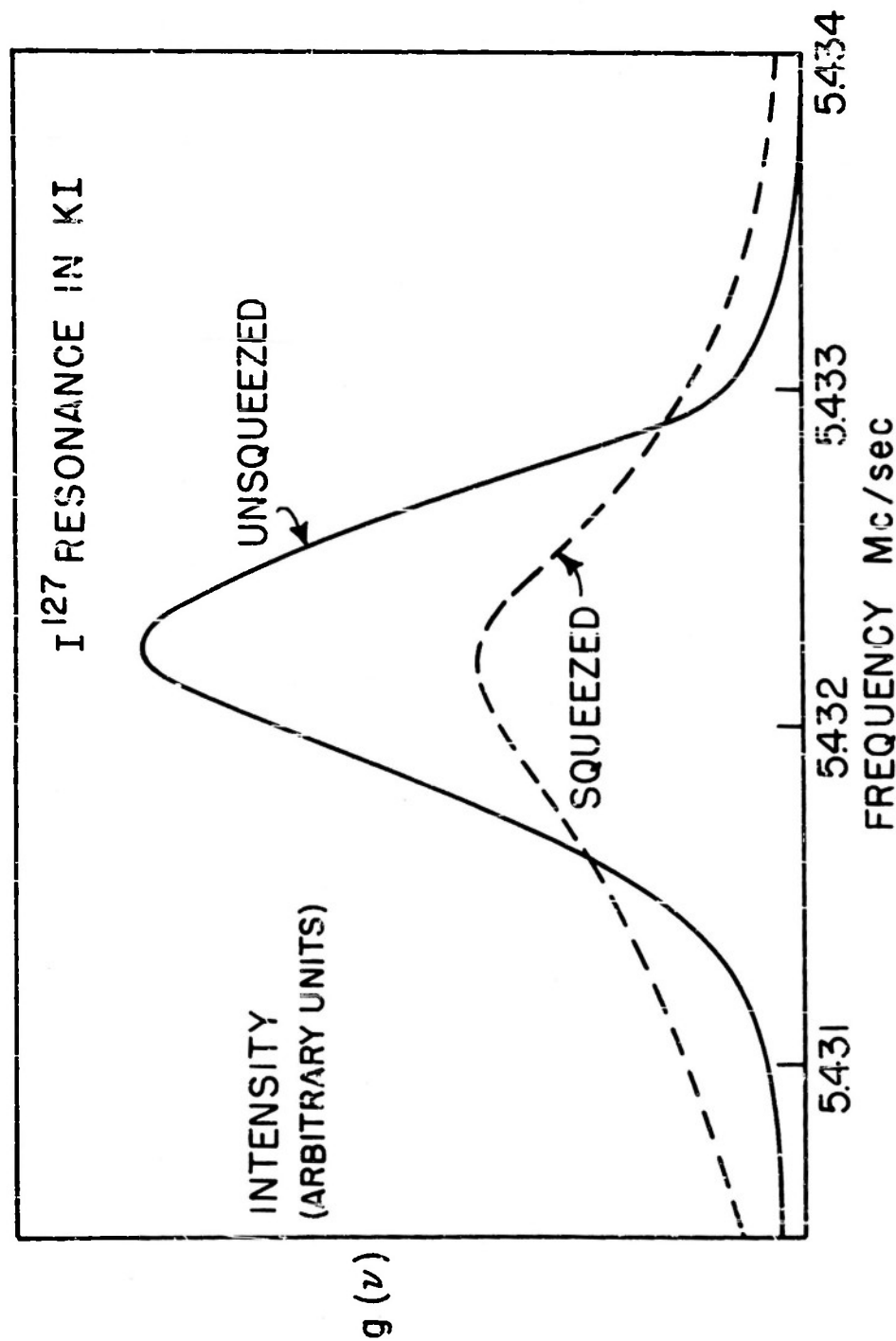
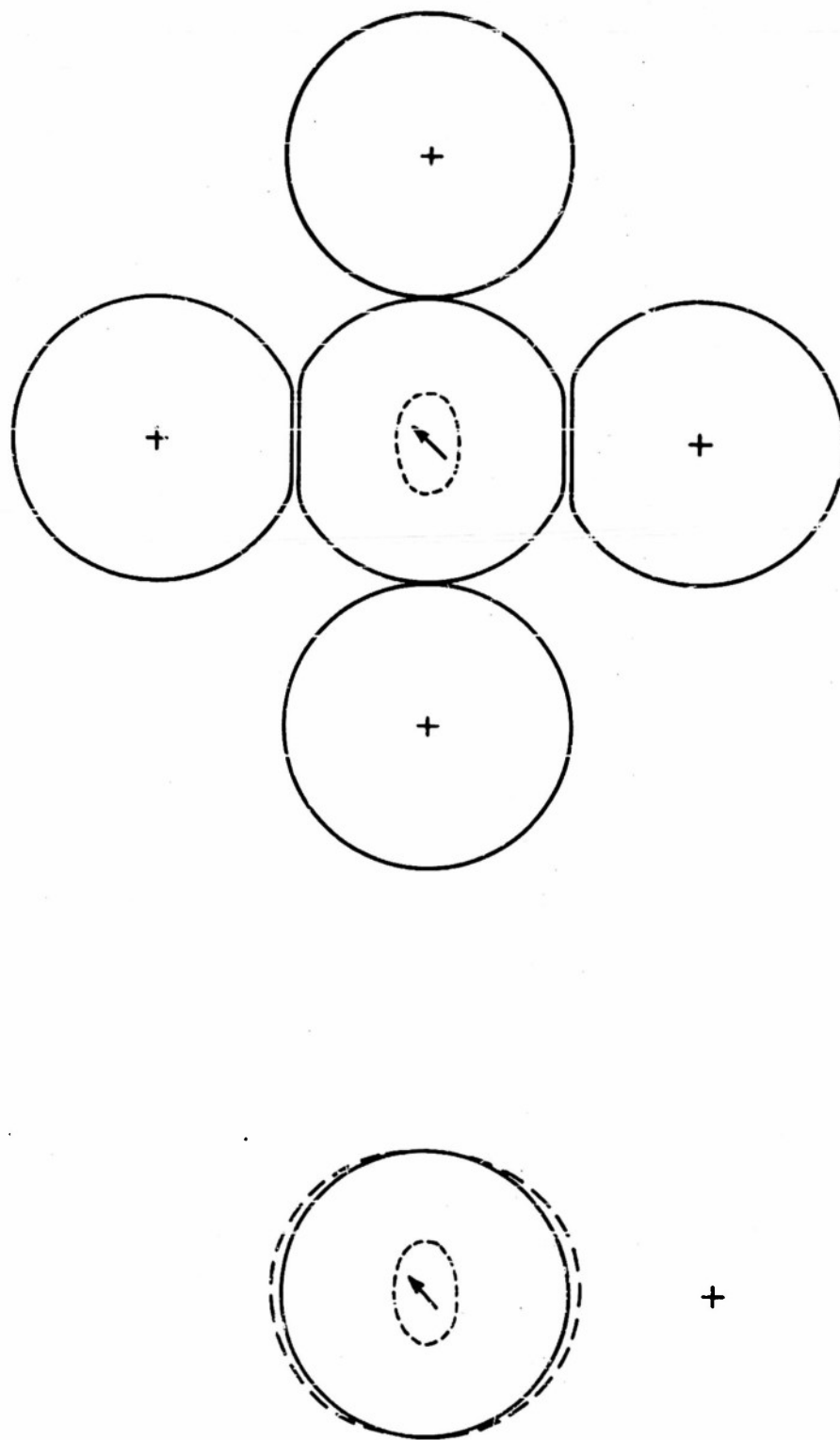


Fig. 11. Second-order broadening of the I<sup>127</sup> resonance absorption in a plastically deformed KI single crystal. A 3 per cent reversible effect due to elastic deformation was superimposed on the irreversible effect, arising from a 22 per cent plastic deformation along the 1,0,0 axis (Watkins).

# DEFORMATION OF ELECTRON DENSITY NEAR NUCLEUS



(a) BY EXTERNAL CHARGE

(b) BY ION CORE INTERACTION

Fig. 12. Schematic diagram of the antishielding of the quadrupole interaction. (a) The gradient of a bare external charge is multiplied by the deformed electron distribution near the nucleus. (b) Multiplication of the deformation near the nucleus is also the main cause of the interaction in the case of lattice strains.

The corresponding change in resonant frequency of the transition between the nuclear spin levels  $m_I$  and  $m_I - 1$  is consequently in first-order perturbation

$$h\Delta\nu = + (2m - 1) (3 \cos^2 \theta - 1) \frac{18 e^2 Q \lambda}{8I(2I - 1) r a^2} \quad (12)$$

A good measure for the magnitude of the perturbation is obtained by calculating its second moment as a radial average over the deformed cylinder around a dislocation line. The lower limit of integration is rather arbitrarily chosen as  $r_i = 3a$ . The second moment will depend only logarithmically on this cut-off radius. Inside this radius the atomic displacements cannot be calculated from a continuum elastic theory. Moreover the relative fraction of nuclei inside this radius is small, and they contribute to the far wings of the absorption line. Their signal will escape observation and a cut-off is dictated by this physical interpretation. The outer radius is chosen so that the cylinder has the average volume per dislocation line,  $\pi r^2 = c^{-1}$ , where  $c$  is the number of dislocation lines, crossing  $1 \text{ cm}^2$  of normal area. The second moment of the line is then found to be

$$(\delta\nu)^2 = \frac{4}{5} \left[ \frac{(2m-1) 3 e^2 Q}{8I(2I-1)h} \right]^2 (6\lambda)^2 a^{-4} \int_{3a}^{(\pi c)^{-1/2}} r^{-2} r dr \left| \int_0^{(\pi c)^{-1/2}} r dr \right.$$

This result differs by a factor  $3/\pi^2$  from a more rigorous formula derived by Watkins for the effect of six neighboring ions due to shear strain in the K Br type lattice.

$$(\delta\nu)^2 = \frac{432}{5\pi} \left[ \frac{3e^2 Q(2m-1)}{8I(2I-1)a^3 h} \right]^2 \lambda^2 c a^2 \ln(1/9 ca^2) \quad (13)$$

random  
disl.

Watkins took proper account of the angular dependence of the strain around the dislocation line [26] and, averaged over a statistical distribution of dislocations with random orientation,  $ca^2$  is the probability that a dislocation line passes through a given lattice point. Present uncertainty in the anti-shielding factor  $\lambda$  and the experimental data hardly justify a more detailed

calculation, and Watkins's formula may be used equally well for edge and screw dislocations. The phenomenological factor  $\lambda$  is a function of the ion and the lattice in which it is embedded. Its order of magnitude is not necessarily the same as the Sternheimer factor  $1 + |\gamma_{\infty}|$  which describes the distortion of an ion core by an external charge and is a constant for a given ion. Watkins found that his results were consistent with  $\lambda = 10$  for the bromine and iodine resonance in KBr and KI, with  $c = 6 \cdot 10^8 \text{ cm}^{-2}$  for the pure crystals and  $c = 10^{10} \text{ cm}^{-2}$  for the plastically deformed crystals. It would be of interest to compare the values of  $\lambda$  for anions and cations in the same crystal e.g., in NaBr. It is to be expected that  $\lambda$  should be considerably smaller for  $\text{Na}^+$  than for  $\text{Br}^-$ .

An effect of dislocations on the satellites has been found in metallic copper [11]. The specimen consisted of 320 mesh copper filings to permit the radiofrequency field to penetrate the individual particles. When cold-worked filings were annealed the peak intensity of the resonance could be increased by a factor 2.5. By annealing  $g_s(\nu_{\max})$  in equation (11) changes from essentially zero to  $g_c(\nu_{\max})$ , which remains the same. For intermediate stages of anneal intermediate peak intensities  $g(\nu_{\max})$  were recorded. In the well-annealed crystals the density of dislocations is so low that first-order quadrupole interactions appear to be negligible. A value for the antishielding parameter  $\lambda = 60$  for copper will be used, which is derived from experiments to be described later. This value is substantially larger than Sternheimer's value  $1 + |\gamma_{\infty}| = 9.7$ . It should be remembered that the two quantities are not strictly comparable, and  $\lambda$  will be larger if there is considerable ion core overlap. In addition there may be a contribution to the electric field gradient in the metal from distorted valence electron wave functions.

An upper limit for the density of dislocations, which are assumed to be randomly distributed, can be obtained from the fact that the first-order quadrupole broadening is less than the dipolar broadening  $\left\{ \langle \delta\nu \rangle_{\text{dipolar}}^2 \right\}^{1/2}$  ( $2.5 \times 10^3$ ) cps. Equation (13) then yields an upper limit for the density of dislocations in annealed copper  $c < 10^7 \text{ cm}^{-2}$ . This figure may be somewhat too small, because  $\lambda$ 's estimate is rather high. It is in fair agreement with data derived from the width of X-ray diffraction spots on the assumption of a random arrangement of dislocations.

Instead of a random distribution of dislocations, one can assume

dislocation walls and mosaic boundaries. Usually the stress field will be very small at some distance from the wall and such arrangements are not detected by the nuclear resonance method. Their effects are of course detectable by X-ray techniques. It is possible that the first stages of polygonization will show as an increase in  $g(\nu_{\max})$  of the nuclear resonance, before these are detectable by X-ray diffraction.

There was no evidence for second-order quadrupole effect on the central component in the cold-worked copper. This is not unreasonable, for the calculation of the broadening of the central component, which vanishes in first approximation according to equation (13), in the stress field around a dislocation yields a result which depends very sensitively on the cut-off radius  $r_i$

$$\langle (\delta\nu)_c^2 \rangle_{av} \approx \lambda^4 \left[ \frac{e^4 Q^2}{h^2 a^6 \nu_0} \right]^2 \frac{1}{4} c a^2 \left( \frac{a}{r_i} \right)^2$$

The second-order interaction decreases rapidly with the distance, and the second moment gives no satisfactory physical description. The nuclei are either so close to the dislocation that their contribution to the central component is smeared out over a large frequency range and is thus unobservable, or else they are far enough away - and this is the majority - that they produce a nearly unbroadened central line. The central component resonance of nuclear spins a distance  $r$  from the dislocation line will be spread out over a frequency range

$$\Delta\nu_{c, \text{extr}} = \frac{25}{64} \frac{2I + 3}{4I^2(2I - 1)} \frac{e^4 Q^2}{h^2 \nu_0 a^4 r^2} \lambda^2 \quad (14)$$

If the density of dislocations is  $c$ , a fraction  $cr^2$  of the nuclei will be inside a radius  $r$  from a dislocation line.

From the disappearance of the satellites in cold-worked copper we may conclude that  $(\delta\nu)_c^2$  is larger than  $(2.5 \times 10^4)^2$ . Otherwise they would have been observable. With the data of Table I and

Table I

I	$\nu$ cps for $R_0 = 5500$ gauss	Q	Goldschmidt Atomic Radius	$\lambda$	Dipolar Sec. Moment $(5\nu)^2$
Al $^{27} \frac{5}{2}$	$6.1 \times 10^6$	$0.156 \times 10^{-24} \text{ cm}^2$	$1.42 \times 10^{-8} \text{ cm}$	$4.04 \times 10^{-8} \text{ cm}$	$(3.4 \times 10^3)^2 \text{ sec}^{-2}$
Cu $^{65} \frac{3}{2}$	$6.7 \times 10^6$	$-0.145 \times 10^{-24}$	$1.28 \times 10^{-8}$	$3.60 \times 10^{-8}$	$(2.5 \times 10^3)^2$

$\lambda = 60$ , equation (13) yields  $c > 3 \times 10^8 \text{ cm}^{-2}$  for cold-worked copper. On the other hand, the central component appears to be unaffected. The central component is spread over a frequency range  $\Delta\nu$  equal to the root of the dipolar second moment at a radius  $r = 0.64 \times 10^{-6} \text{ cm}$  according to equation (14). Assuming that less than 10 per cent of the nuclear spins are closer to a dislocation line, an upper limit for the density of dislocations is found  $c < 2 \times 10^{11} \text{ cm}^{-2}$ . A value  $c = 10^{11} \text{ cm}^{-2}$  is compatible with other experimental evidence for cold-worked copper, e.g., from stored energy and X-ray data [27].

In pure aluminum no decrease in intensity after cold work was observed. This observation is also in agreement with X-ray data which show very little broadening of diffraction spots after cold work [28], as compared to copper. Presumably the dislocations in pure aluminum are stacked in an ordered arrangement such that there is destructive interference of the stresses at large distances from the dislocation walls. In fact, theory predicts that the stress will drop to zero according to the exponential  $\exp(-x/\Delta)$ , where  $\Delta$  is the average spacing of dislocation lines in the wall. This assumption must be preferred over the alternative of self-annealing and over-all low density of dislocations, as the macroscopic mechanical properties of aluminum do change after cold work at room temperature. It would be of interest to investigate the quadrupole broadening in filings worked at liquid air temperature.

The decrease in the maximum of the central component of the copper

resonance by second-order quadrupole interaction is counteracted by a slight decrease of the second moment of the dipolar interaction, when the satellites are displaced. This may seem strange at first. In the perfect cubic lattice of well-annealed copper Van Vleck's formula equation (1) is valid. For the  $\text{Cu}^{65}$  resonance, e.g., the first term extends over all other  $\text{Cu}^{65}$  nuclei, the second term over  $\text{Cu}^{63}$  nuclei. When the four spin levels of the  $\text{Cu}^{65}$  nucleus cease to be equidistant, the first term is no longer correct. In its derivation that part of the dipolar interaction was retained in which a pair of spins  $i$  and  $j$  does not change its total  $m$ -value, or terms for which  $\Delta m_i = \Delta m_j = 0$  or  $\Delta m_i = -\Delta m_j = \pm 1$ . In the cold-worked copper part of the dipolar interaction corresponding to transitions like  $\Delta m_i = \frac{3}{2} \rightarrow \frac{1}{2}$ ,  $\Delta m_j = -\frac{1}{2} \rightarrow \frac{1}{2}$  have to be excluded, since energy is no longer conserved in the presence of quadrupolar interaction. The situation in which this interaction vanishes accidentally because of the angular factor  $(3 \cos^2 \theta - 1)$  is neglected. This omission is less serious, the larger the quadrupole interaction. Furthermore, only transitions produced by the external oscillating field between the levels  $m_I \pm \frac{1}{2}$  are of interest. In equation (1) transitions between all levels were taken into account. Kambe and Ollon [29] have derived a formula for the dipolar broadening of the central component alone. For  $I = \frac{3}{2}$  the proper numerical factor is now  $\frac{27}{40}$  instead of  $\frac{3}{4}$  in the first term and for  $I = \frac{5}{2}$  the new factor is  $\frac{107}{105} \times \frac{3}{4}$ . The factor of the second term remains unchanged.

There are also some changes in the establishment of thermal equilibrium, if the levels are unequally spaced. In metals the important relaxation mechanism consists of magnetic dipole transitions caused by interaction with the conduction electrons. The set of differential equations for the population in each of the sublevels is solved in the appendix. The result is that in the steady-state method of saturation the maximum of the imaginary part of the susceptibility drops to half its value for  $\frac{1}{4} \gamma^2 H_{rf}^2 T_1 g(\nu_{\max}) = 1$ , i.e., the same result as in the absence of quadrupole broadening;  $T_1$  is the relaxation time for the case of equidistant levels. The recovery to thermal equilibrium is, however, appreciably different, if the  $m$ -levels are unequally spaced. Suppose that the population in the  $m_I = \frac{1}{2}$  and  $-\frac{1}{2}$  levels has been equalized by complete saturation. The recovery of the Boltzmann distribution for these two levels is described by a linear combination of two exponentials with characteristic times of  $T_1$  and  $\frac{1}{5} T_1$ . The recovery of the signal in small

radiofrequency fields after saturation of the central component with  $I = \frac{3}{2}$  is given by

$$g_c(t) = \left( -\frac{2}{5} e^{-t/T_1} - \frac{3}{5} e^{-6t/T_1} + 1 \right) g_c$$

The initial recovery rate is four times as fast as in the absence of quadrupole perturbation; and 9 times as fast for  $I = \frac{5}{2}$ . This rate is observed, e. g., in the pulse or spin-echo method if only the central component is flipped over. Considerable care in the analysis of the recovery of the spin system is required in each individual case.

#### B. Vacancies and interstitials

The calculations of the nuclear quadrupole interaction around a static vacancy or interstitial will be along the same lines as the calculations for chemical impurities described in the next paragraph. There is a good reason not to treat it here, as these effects become important only for concentrations higher than 0.1 per cent. Such high concentrations of vacancies normally occur only at high temperatures close to the melting point, where there is at the same time a rapid rate of diffusion. In the case of severe radiation damage produced at low temperature a static distribution of high vacancy and interstitial concentration could be obtained. For the treatment of this case we refer to the next section. Here the time-dependent quadrupole effect in a crystal with an appreciable vacancy concentration at elevated temperatures is discussed. We can describe the diffusion as a random motion of the vacancies through the lattice. Assume for the sake of simplicity that the electric field is  $q$  whenever a nucleus is adjacent to a vacant site and zero elsewhere. A more rigorous treatment would obviously include a summation over a distribution of  $q$ -values. The probability for a nucleus to be next to a vacancy is

$$p(0) = -ze^{-E_{\text{vac}}/kT}$$

where  $z$  is the number of neighboring sites and  $E_{\text{vac}}$  is the energy required for the formation of a Schottky vacancy. The probability that a given nucleus is still next to the same vacancy after a time  $t$  is  $\exp(-t/\tau)$  where

$$\tau^{-1} = (z-1) \nu_{at} e^{-\bar{E}_{act}/kT}$$

is the jumping frequency of the vacancy to any of the  $z-1$  other neighboring positions. The correlation function of the time-dependent electric field gradient is consequently

$$\overline{q(t)q(t+t')} = q^2 z e^{-E_{vac}/kT} e^{-t'/\tau}$$

and the quadrupole contribution to the transition probability or the inverse nuclear relaxation time is consequently proportional to

$$\left(\frac{1}{T_1}\right)_Q \propto \frac{h^{-2} e^4 Q^2 q^2 z e^{-E_{vac}/kT} \tau}{1 + 4\pi^2 \nu_o^2 \tau^2}$$

For  $\tau \ll \nu_o^{-1}$

$$\left(\frac{1}{T_2}\right)_Q = \left(\frac{1}{T_1}\right)_Q \approx h^2 e^4 Q^2 q^2 \frac{z}{z-1} \nu_{at} e^{(-E_{vac} + E_{act})/kT} \quad (15)$$

In this most important case of fast diffusion the relaxation by quadrupole coupling contains a different combination of energies in the exponent than the dipolar interaction, which contains  $(E_{vac} + E_{act})$  as does the diffusion constant. If the quadrupole interaction is dominant at high temperatures,  $E_{vac}$  and  $E_{act}$  can be determined separately with resonance methods. The condition  $\tau \ll \nu_o^{-1} \approx 10^{-7}$  sec will usually be satisfied only quite close to the melting point. At lower temperatures where  $\tau \gg \nu_o^{-1}$ , the quadrupole interaction will usually be negligible compared to magnetic interactions. The same treatment holds for interstitials except that  $z/z-1$  is then replaced by unity in equation (15). No experimental evidence of the effect described by this formula is known. It could occur both in metals and insulators.

The quadrupole interaction in liquids and its contribution to the relaxation mechanism is well established [30,31]. One could consider this as a limiting case of the foregoing in which the concentration of vacancies is large and in-

dependent of the temperature.  $T_1$  depends on the temperature only through the jumping time  $\tau$  which is proportional to  $(\eta/T)$  where  $\eta$  is the viscosity.

### C. Foreign atoms

The influence of foreign atoms on the electric field gradient is two-fold. One can distinguish between charge and size effects. In the first place one can imagine an ion in an ionic crystal replaced by another of the same size but differing by an electronic charge  $e$ . A vacancy will also act as an extra charge, equal and opposite to the charge of the ion normally occupying the lattice site. Some distance  $r$  away from the impurity atom the quadrupole interaction with a nucleus will cause a change in the resonant frequency between the  $m$  and  $m - 1$  spin level

$$h \Delta \nu = (2m-1) \frac{3 e^2 Q}{8I(2I-1)} \frac{1 + |\gamma_{\infty}|}{\epsilon r^3} (3 \cos^2 \theta - 1) \quad (16)$$

where  $\epsilon$  is the dielectric constant,  $\theta$  the angle between the radius vector  $r$  and the external magnetic field, while  $(1 + |\gamma_{\infty}|)$  is the antishielding factor calculated by Foley and collaborators. In a metal an impurity atom of the same atomic volume but different valency will, in the free electron approximation, produce a screened Coulomb field [12] around it with screening parameter  $K$ , and the change in splitting of the spin levels due to the quadrupole interaction will be given by

$$h \Delta \nu = \frac{(2m-1) 3 e^2 Q}{8I(2I-1) r^3} (1 + Kr + \frac{1}{2} K^2 r^2) e^{-Kr} (1 + |\gamma_{\infty}|) (3 \cos^2 \theta - 1)$$

Take the square of the displacement and average over a sphere of volume  $\frac{4}{3} \pi r^3 = C^{-1}$ , where  $C$  is the impurity concentration, to obtain the second moment of the broadened satellites. The first moment is zero because of the angular dependence. In an ionic crystal the second moment will be given by

$$\overline{(\Delta \nu)_{m \rightarrow m-1}^2} = \frac{4}{15} (2m-1)^2 \frac{9 e^4 Q^2}{64 I^2 (2I-1)^2 4 r_i^3 \epsilon^2 h^2} C \left\{ 1 + |\gamma_{\infty}| \right\}^2$$

This result depends very sensitively on an inner cut-off radius  $r_i$ . The fourth moment would vary as  $r_i^{-9}$ . There are a few very large contributions to the moments from nuclei in the immediate neighborhood of the impurity, while the majority causes only a relatively small broadening. Under these circumstances a useful physical description is again obtained by considering the nuclei in a spherical shell of radius  $r$  around the impurity. The signal from these nuclear spins is spread out over a frequency interval given by equation (16), if we substitute 3 for the range of values of  $3 \cos^2 \theta - 1$ . When this frequency range exceeds a certain critical value, which depends on the experimental sensitivity, we may say that the contribution of these nuclei is unobservable, because it is spread out over such a broad frequency range. A practical value of this limit is determined by the signal-to-noise ratio and is about 25 kc/s for the experiments on the copper and aluminum resonance described in this paper. A critical radius  $r_{cr}$  is defined by taking  $\Delta\nu$  in equation (16) of the same order of magnitude as the dipolar broadening. The nuclei inside this sphere contribute ~~only to the~~ unobservable wings of the resonance signal; nuclei outside the sphere give an essentially unbroadened signal. Clearly this reduction of the quadrupole interaction to an "all or nothing" effect is a great oversimplification. Its only merit is its usefulness in discussing existing experimental data on the maximum absorption as a function of impurity content. When more precise experimental data on the complete line shape become available, the analysis can be made more complete. The contribution of the nuclear spins in each spherical shell has the shape shown in Fig. 9. These contributions should be added to obtain the resultant line form.

In addition to the electric field gradient produced by the extra charge of vacancy, interstitial or foreign atom, there is the effect from the stress field around the imperfection. The strain deformation around a spherical inclusion in an elastic medium falls off as the inverse cube of the distance [32]. If the foreign atom and solvent atom have radii  $a_i$  and  $a_o$  respectively, the relative displacement of two ions a distance  $r$  from the impurity has the order of magnitude

$$\Delta a_c = (a_i - a_o) a_o^3 r^{-3}.$$

Introducing the same antishielding factor  $\lambda$  as in the discussion of ion core

distortion around a dislocation, we obtain

$$h \Delta \nu = + \frac{18 e^2 Q(a_i - a_o)}{r^3 a_o} \lambda \frac{(2m-1)}{8l(2l-1)} (3 \cos^2 \theta - 1) \quad (17)$$

This shift has to be added to the result (16) before calculating the second moment of the satellites by the quadrupole interaction in an ionic crystal.

It would be of interest to study these charge and size effects in detail with controlled impurities in ionic crystals. Reif has very recently observed such quadrupole effects on the bromine resonance in AgBr, containing  $\text{Cd}^{++}$  ions. Presumably there will be a corresponding number of  $\text{Ag}^+$  vacancies to retain over-all neutrality. At low temperatures the  $\text{Cd}^{++}$  ion and the vacancy will be associated [33]. At high temperatures they are independent impurities. The quadrupole broadening in such a crystal will undoubtedly change with temperature and the dissociation process could in principle be followed in some detail. While this suggestion was written in the manuscript, the author was unaware that Reif had already discovered such effects and their explanation had already been given by Cohen and Reif [34].

### C.1 First-order quadrupole effects in metals

In a metal the electric field is so strongly shielded ( $K = 2.10^8 \text{ cm}^{-1}$ ) that the ion deformation by strains gives the only contribution to quadrupole broadening. Equation (17) should be used. In Fig. 14 the maximum absorption of the satellites of  $\text{Al}^{27}$  in an Al-Mg alloy observed by Rowland [35] is plotted as a function of Mg-concentration. Cold-worked filings display at first the combined effect of impurities and dislocations. The fact that in cold-worked impure aluminum the dislocations are not annealed out at room temperature is in agreement with other metallurgical observations. According to Cottrell [36] the dislocations are locked to an "atmosphere" of impurity atoms. On annealing at higher temperatures the concentration of dislocations becomes too small to give an observable contribution. The first-order quadrupole effect of the impurities is then retained. We may subtract from the total observed absorption  $g(\nu_{\text{max}})$  the central component contribution  $g_c(\nu_{\text{max}})$  and plot the maximum intensity of the satellites

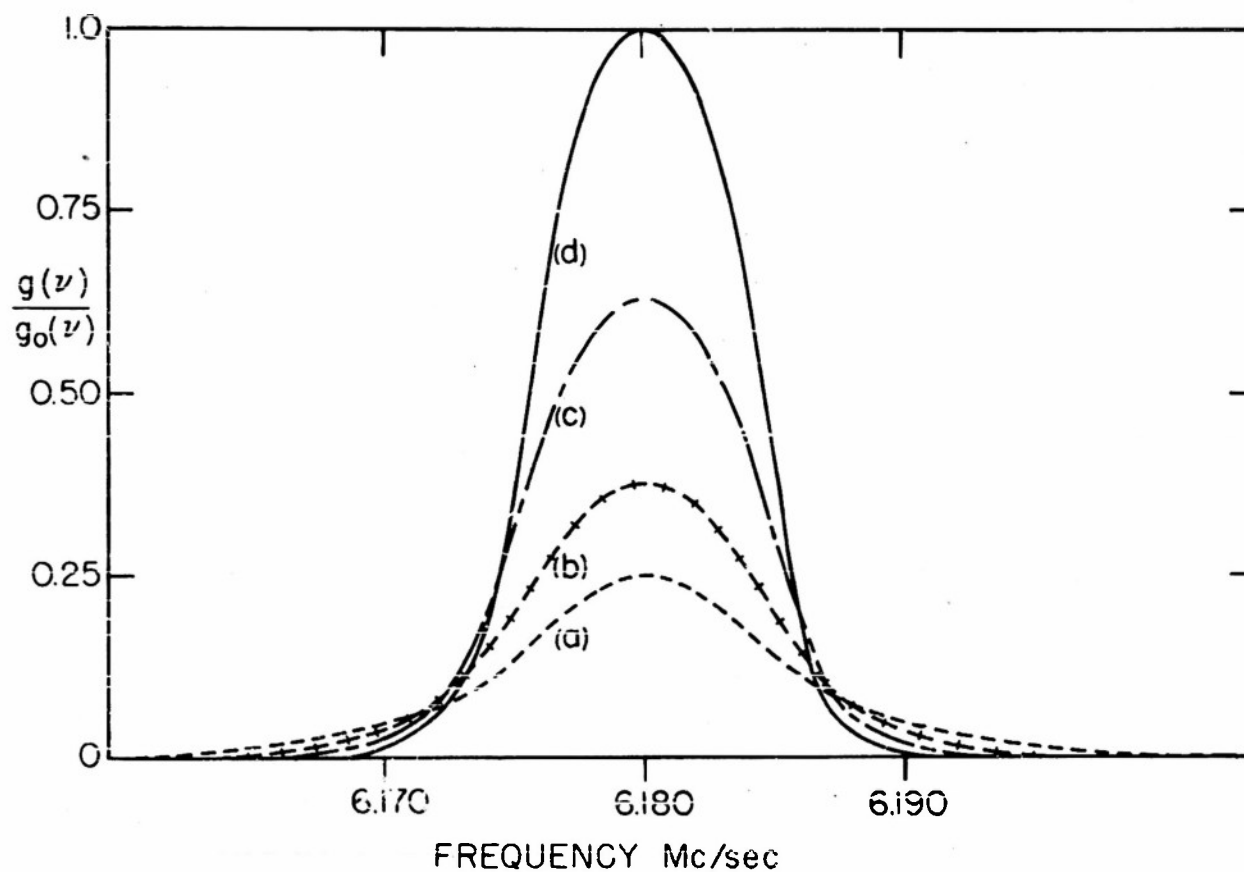


Fig. 13. The line shape of the  $\text{Al}^{27}$  resonance in aluminum alloy with 0.64 atomic per cent magnesium. (a) after filing at room temperature, (b) after filing and 87 hours at  $250^\circ\text{C}$ , (c) after filing and 2 hours at  $480^\circ\text{C}$ , (d) the absorption in pure aluminum, included for comparison. The peak intensity increases, as the density of dislocations decreases with annealing. The remaining reduction of (c) as compared to (d) is the effect of the Mg-impurities alone. (Rowland).

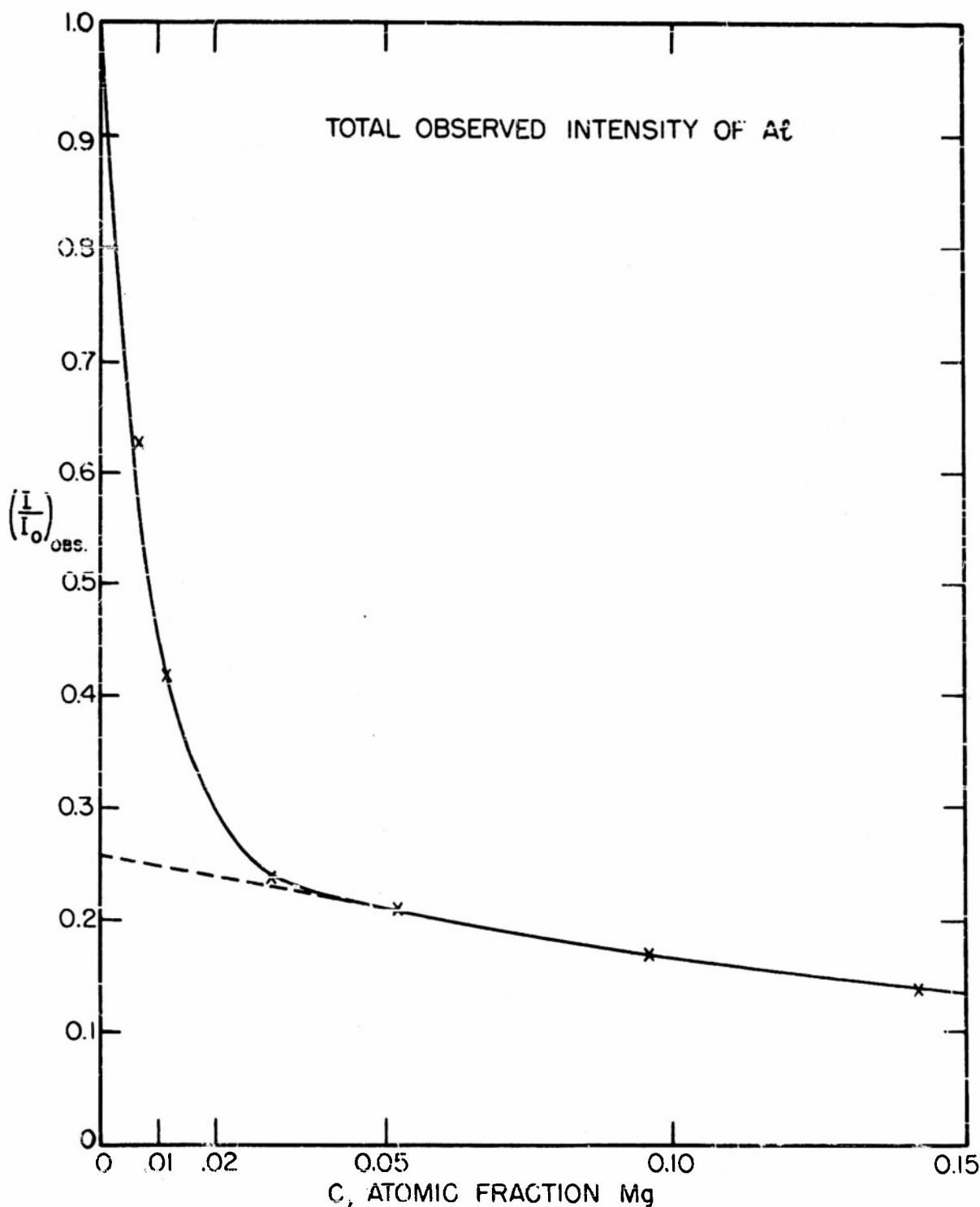


Fig. 14. The peak intensity of the  $\text{Al}^{27}$  resonance in  $\text{Al-Mg}$  in annealed alloys as a function of the Mg-concentration at room temperature. The satellite peak intensity decreases rapidly. At 4 atomic per cent Mg only a contribution of the central component remains. This component extrapolates to 0.257 in pure aluminum, the theoretical value for  $I = 5/2$ . The alloys with high Mg-concentration were obtained by quenching the powdered specimen from high temperatures, where the solid solubility is high. (Rowland).

$g_s(\nu_{\max})$  in the annealed alloy as a function of the Mg-concentration on a double logarithmic scale. The result is a straight line. This finds a natural explanation in terms of the "all or nothing" language introduced earlier. If there is no Mg-atom inside the critical radius the aluminum nucleus will contribute to the satellite signal; otherwise not. The Mg-atoms are supposed to be distributed at random over the lattice, which is certainly correct at these low concentrations. Each lattice has a probability  $C$  to be occupied by an Mg atom, where  $C$  is the relative Mg concentration. The number of lattice sites inside the critical radius is

$$N = \frac{4\pi}{3} r_{cr}^3 / v_a$$

The probability that an  $Al$  nucleus has no Mg atom inside the critical distance  $r_{cr}$  is consequently  $(1-C)^N$  and the maximum intensity of the satellite signal for  $I = \frac{5}{2}$ , normalized per  $Al$  atom

$$g_s(\nu_{\max}) = g_{s,0}(\nu_{\max}) (1 - C)^N \quad (18)$$

Experimentally it is found that  $N = 130$ . Since  $N$  is so large the cut-off is not as sharp as we have assumed. It is somewhat surprising that the experimental results can be so well described in this fashion.

The introduction of zinc in the aluminum lattice gives a reduction of the satellites, shown in Figs. (15) and (16), which are well described by  $N = 98$ . The cut-off radius lies between the sixth and seventh near neighbor in the face-centered cubic lattice. The ratio of quadrupole interaction at these two sites is  $q_1/q_2 = (r_7/r_6)^3 = 0.79$ . This fraction is not large and the cut-off is not very sharp. If the experimental precision were increased - e.g., by increasing the absorption intensity through cooling to liquid helium temperature - a more precise analysis of the strain field could be made. Wings of the satellite away from the central peak have already been observed, but a precise evaluation of the line shape has not yet been made.

It is not surprising that the effective cut-off radius for Zn is smaller, as the Zn atom has more nearly the same size as the  $Al$ -atom than magnesium. Since the gradient at the cut-off radius must be the same, it follows from equation (17), that

$$\frac{a_{\text{Mg}} - a_{\text{Al}}}{a_{\text{Zn}} - a_{\text{Al}}} = \left( \frac{r_{\text{cr, Al}}}{r_{\text{cr, Mg}}} \right)^{-3} = \frac{130}{98} = 1.3$$

This is in poor agreement with tabulated values of Hume-Rothery [36], which give 3.5 for this ratio.

## C.2 Second-order quadrupole effects

The broadening of the central component can be analyzed along similar lines. Since this interaction will drop off with the inverse sixth power of the distance from the impurity, the second moment of this interaction averaged over the whole crystal will give even less relevant information than for the first-order effect. The second moment would be proportional to the inverse ninth power of inner cut-off radius. The nuclear spins at a distance  $r$  from the impurity will give a contribution to the central component which has the shape displayed in Fig. 10 with a distance between the extremes given by

$$\Delta \nu_{\text{c, ext.}} = \frac{25}{64} \frac{2I + 3}{4I^2 (2I - 1)} \frac{e^4 Q^2}{h^2 \nu_0 r^6} \left( \frac{a_i - a_o}{a} \right)^2 \lambda^2 \quad (19)$$

Assuming that the inverse cube law for the strains holds also in the immediate neighborhood of the impurity, this frequency range at first, second and third nearest neighbors in a face-centered cubic lattice has the ratios 27: 3.37: 1. It is therefore quite possible that this range for third nearest neighbors is only a fraction of the dipolar broadening, while it is appreciably larger than the dipolar interaction for nearest and next nearest neighbors. The nuclear spins which have an impurity in one of these  $z$  neighboring sites would then give an observable effect, while other nuclei would contribute to an otherwise unchanged central component. In other words a sharp cut-off may now be expected with more justification than in the satellite case. The maximum intensity of the central component if  $I$  is an odd half-integer is consequently given by

$$g_{\text{c}}(\nu_{\text{max}}) = g_{\text{c},0}(\nu_{\text{max}}) (1 - C)^z \quad (20)$$

where  $C$  is the relative impurity concentration of the solute atoms. For a face-centered cubic lattice,  $z$  may assume one of the values 0, 12 or 18,

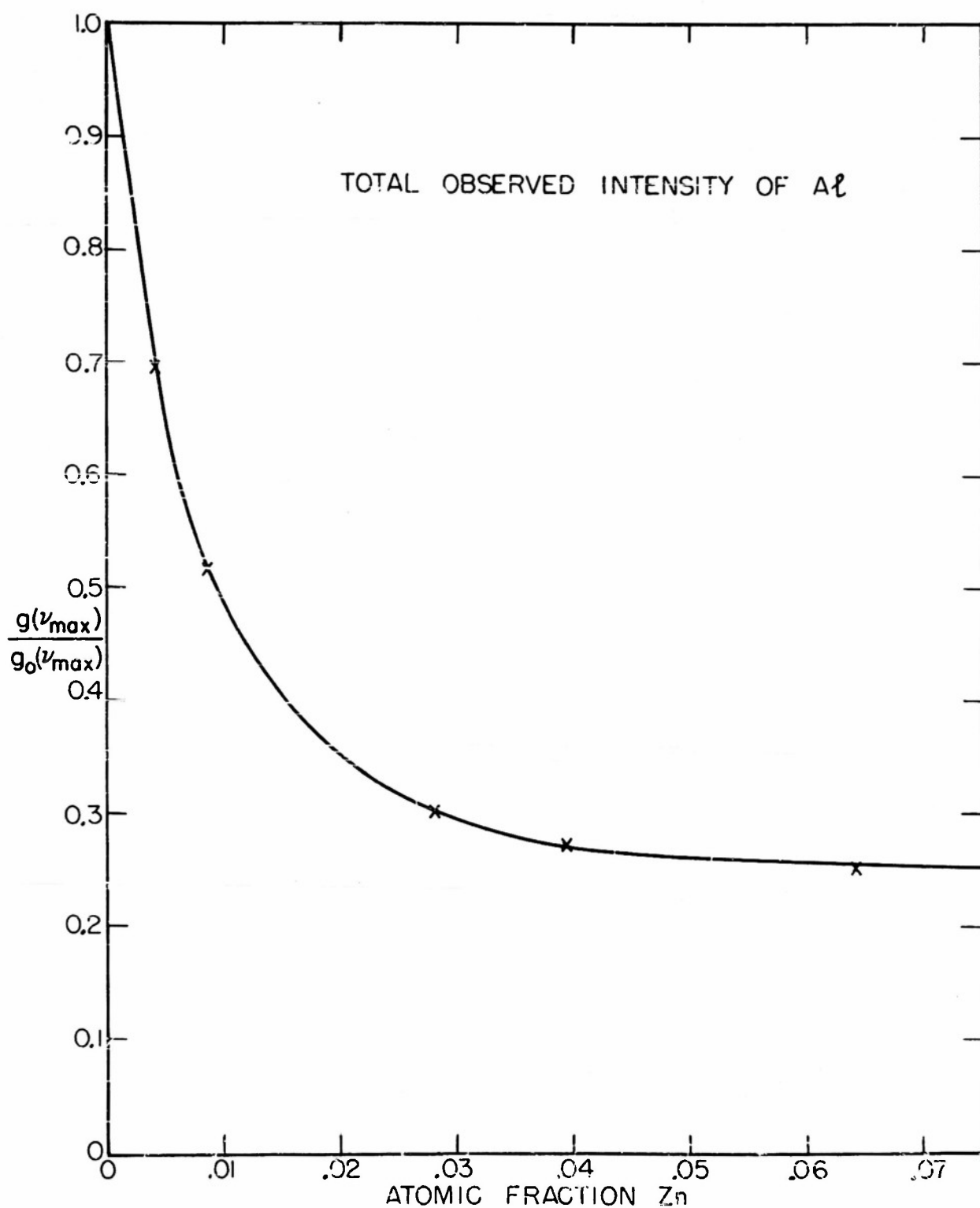


Fig. 15. The peak intensity of the  $Al^{27}$  resonance in  $Al-Zn$  alloys at room temperature, at 6.18 Mc/s. The satellites are washed out, the central component remains unchanged. (Rowland).

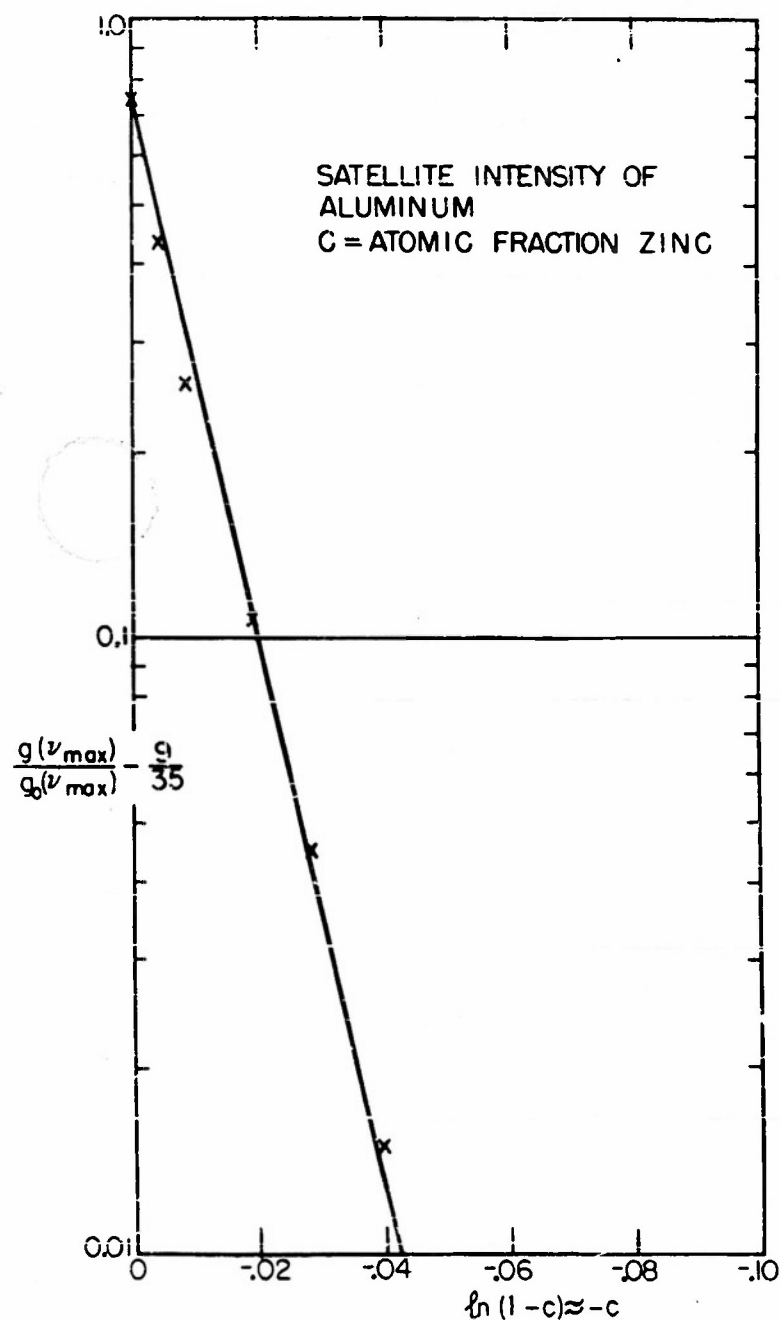


Fig. 16. A double logarithmic plot of the peak intensity of the satellites alone

$$\frac{g(v_{\max})}{g_0(v_{\max})} - \frac{9}{35} = \frac{26}{35} \frac{g_s(v_{\max})}{g_{s,0}(v_{\max})}$$

for the  $\text{Al}^{27}$  resonance in  $\text{Al-Zn}$  alloys as a function of the Zn-concentration. The straight line has a slope of 98. The data have been obtained from Fig. 15 by subtracting the effect of the central component. (Rowland).

etc. and in a body-centered cubic lattice 0, 6 or 14. The data on the central component are most conveniently taken in cold-worked samples. The contribution of satellites to the signal is then effectively eliminated by the large density of dislocations so that no correction for them is necessary. In this way the data in Fig. 17 for the central component in  $\alpha$ -brass have been obtained [11]. Indeed it was found that  $z = 18$  for the copper resonance in  $\alpha$ -brass, and  $z = 0$  for the  $Al^{27}$  resonance in the aluminum zinc alloy.

These numbers depend on the resonance frequency  $\nu_0$ . In very high external magnetic fields the second-order quadrupole interaction will tend to zero, and so does the critical radius. For lower frequencies the  $Al^{27}$  resonance in the aluminum zinc system may give  $z = 12$ . It would be interesting to follow nearly discontinuous changes in  $z$ , as  $\nu_0$  is increased or decreased. At very low fields the quadrupole interaction might extend to third nearest neighbors etc. and a detailed study of this kind will give information about the stress field in the immediate neighborhood of the impurity and will show any deviation from the continuum theory which might exist on an atomic scale.

From the first-order and second-order broadening values for the product  $\lambda(a_i - a_0/a)$  may be derived. A value  $(a_i - a_0/a) = 10$  per cent will be used for  $\alpha$ -brass, and other pertinent data appeared in Table I. If we assume that the quadrupolar spread in frequency  $\Delta\nu_{c,extr}$  is equal to the dipolar broadening  $\langle(\delta\nu)^2\rangle^{1/2}$  for third nearest neighbors, and 3.37 times as large for second nearest neighbors, we find  $\lambda = 60$  for the copper lattice. This estimate is not very reliable, as the elastic continuum theory is not valid for near neighbors. It is much larger than the Sternheimer antishielding factor. This may be correct as the effects from ion core overlap will be severe in the close-packed copper lattice. This rather large value of  $\lambda$  has been used previously to estimate the density of dislocations in copper.

A more reliable value  $\lambda$  in aluminum may be obtained from the first-order quadrupole effect in aluminum alloys. The critical radius for satellite broadening in the  $Al$ -Zn alloy for  $N = 98$  is  $r_{cr} = 6.5 \times 10^{-8}$  cm. At this radius the mean-square broadening of the inner satellites is assumed to be twice the dipolar second moment. With  $(a_i - a_0)/a_0 = 4$  per cent for zinc

in aluminum, equation (17) yields  $\lambda = 30$ . Probably  $(a_i - a_o)/a$  should be taken somewhat larger and  $\lambda$  correspondingly smaller. The fact that no second-order quadrupole effect is observed in this alloy is consistent with the value  $\lambda(a_i - a_o)/a = 1.2$ . The broadening of the central component for nearest neighbors is  $\Delta\nu_{c,extr} = 2.4 \times 10^3$  cps, or less than the dipolar broadening. The margin is small, however.

In the Al-Mg alloy the strains in corresponding lattice points are larger by a factor 1.3, and in this case the broadening of the central component for nearest neighbors is barely noticeable. The observed line in a quenched alloy containing 14 atomic per cent Mg reproduced in Fig. 18, is a superposition of a line shape of Fig. 10 for Al nuclei which have an Mg-atom as nearest neighbor and an undistorted contribution of other Al nuclei. The asymmetry is much more pronounced in the derivative curve, which was actually recorded. Clearly the second-order broadening from nearest neighbors is small. If we extend the strain theory to the neighbors, the second-order quadrupole interaction should be a factor  $(a_{Mg} - a_o/a_{Zn} - a_o)^2 = (1.3)^2$  larger for magnesium in aluminum than for zinc in aluminum or

$$\Delta\nu_{c,extr} = (1.3)^2 \times 2.4 \times 10^3 = 4.1 \times 10^3 \text{ cps}$$

This is somewhat larger than the dipolar width and a small effect is observed in the magnesium alloy, whereas no effect was observed in the zinc alloy at the frequency of observation  $\nu_o = 6.1 \times 10^6$  cps. Thus the magnitude of the second-order interaction is determined rather precisely.

No noticeable shift of the resonance maximum was found in the aluminum and copper alloys. This is in agreement with the discussion of the Knight shift in alloys illustrated in Fig. 4. Only those copper and aluminum nuclei which are a few interatomic distances away from the solute atoms, contribute to the maximum of the resonance absorption. At these positions the product of density of states and density of the one-electron wave function remains unchanged. The resonance of nuclei adjacent to the impurity, which could show a change of the Knight shift, is unobservable due to quadrupole interaction.

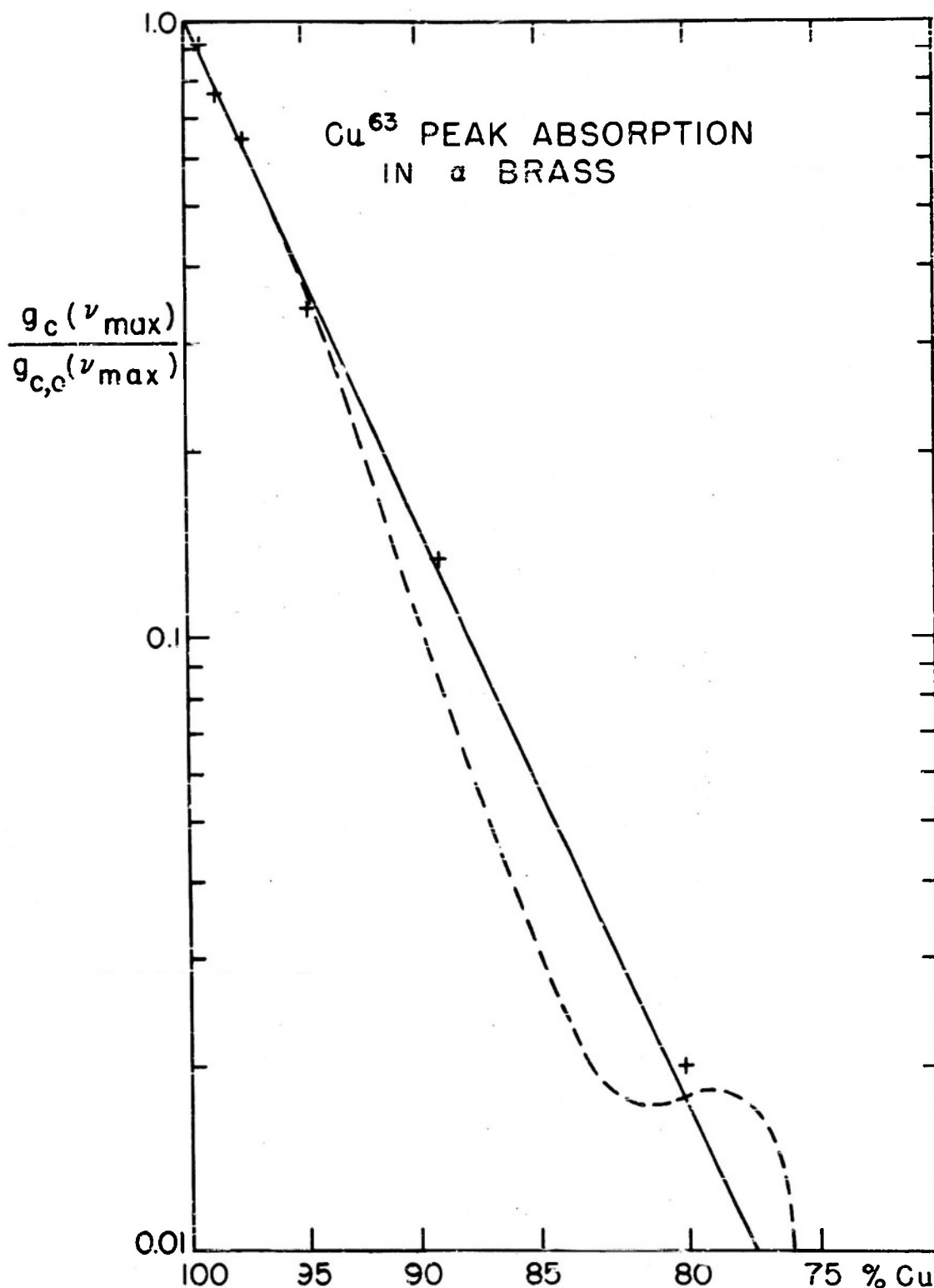


Fig. 17. A double logarithmic plot of the peak intensity of the central component  $g_c(\nu_{\max})/g_{c,o}(\nu_{\max})$  of the  $\text{Cu}^{63}$  resonance in  $\alpha$ -brass, at 6.8 Mc/s. The straight line has a slope 18. The dashed line is the intensity which could be expected in an ordered arrangement where all zinc atoms are contained in one simple cubic sublattice.

### C.3 Precipitation

The values of  $\lambda$  derived for the copper and aluminum lattice were used previously to evaluate the density of dislocation lines in these cold-worked metals. It has been shown how annealing of metals and alloys is generally accompanied by an increase in the maximum magnetic resonance absorption, as the density of dislocations decreases. This effect of temperature treatment should be sharply distinguished from the precipitation of new phases. The latter will frequently lead also to an increase of the resonance signal.

If a precipitate is formed the remaining matrix will contain less solute atoms and the signal  $g(\nu_{\max})$  ought to increase rapidly, as the impurity concentration  $C$  in the original matrix decreases. At first this effect may be obscured by the strains set up by the precipitation process. The intensity  $g(\nu_{\max})$  may be measured as a function of thermal treatment and interpreted in terms of these two effects. No detailed analyses have yet been made, but the occurrence of precipitation in a quenched 14 per cent Mg solution in Al after heating for five days at 250°C is shown in Fig. 18. The asymmetry due to second-order perturbation of the central component disappears, as at the end of the heat treatment the aluminum matrix contains only 3 per cent or 4 per cent Mg atoms and most aluminum nuclei do not have an Mg atom as neighbor. If the quadrupole interaction had been larger ( $\nu_0$  smaller) the effect would have been more pronounced. The increase in intensity after precipitation and annealing should be especially striking if the final matrix would contain so few solute atoms that the satellites would reappear.

### C.4 Order-Disorder

Since the central component signal depends so sensitively on the atomic configuration in the immediate neighborhood of the nucleus with the quadrupole moment,  $g_c(\nu_{\max})$  may be used to investigate short-range order phenomena. Equation (20) derived under the assumption of completely random solution has to be modified, if short-range order is present. We shall first discuss the case of the maximum short-range order which could occur in the face-centered cubic lattice of  $\alpha$ -brass. This is the situation at absolute zero of temperature, if the reaction times would be sufficiently

rapid for it to be established. Clearly this situation will never be attained completely, but this theoretical case will then show what deviations from equation (20) can at most be expected. Only interaction between nearest neighbors is assumed and  $V_{znzn} + V_{cucu} - 2V_{znzc} > 0$  in  $\alpha$ -brass. Precipitation of zinc would occur, if the opposite sign were used. The Zn atoms will tend to stay apart and at sufficiently low temperatures the equilibrium situation will be one in which all Zn's belong to the same simple cubic sublattice of the fcc lattice; in this sublattice the distribution of Zn-atoms will be random. The model could be refined to take into account interaction between next nearest neighbors which are neighbors in the same sublattice. A general theory which covers this case will be mentioned shortly. If the relative concentration of Zn is  $0 < C < 0.25$ , the relative concentration on one sublattice is  $4C$ . The other three sublattices are pure copper. Calculation of the probability that a copper atom has cubic symmetry for the configuration of its 18 neighbors gives for the maximum of the shape function per copper nucleus in this model.

$$g_c(v_{\max})/g_{c,0}(v_{\max}) = \frac{3C}{4(1-C)} (1-4C)^4 + \frac{1-4C}{4(1-C)} \left\{ (1-4C)^6 + (4C)^6 \right\} \quad (21)$$

The first term is the contribution to the intensity of the central component from the three pure copper sublattices. The last term is from the remaining copper atoms. These always have other copper atoms as nearest neighbors; they contribute to the signal if the six next nearest neighbors are either all copper or all zinc atoms. The result is indicated as the dotted line in Fig. 17. For low Zn concentrations the result is the same as for the random solution. At low concentrations the Zn atoms are far away from each other, regardless of whether the state is ordered or disordered. Each Zn atom excludes 18 copper atoms from giving a significant contribution and the intensity drops as  $1-18C$  in this region. At higher concentrations there are fewer Cu nuclei contributing to the signal. Since the Zn atoms tend to stay apart, there are more copper nuclei with a Zn atom in their neighborhood than in the random situation. The peculiar secondary maximum near 20 per cent concentration is caused by configurations with six Zn-atoms as next nearest neighbors. In principle careful measurements of the intensity of the magnetic resonance

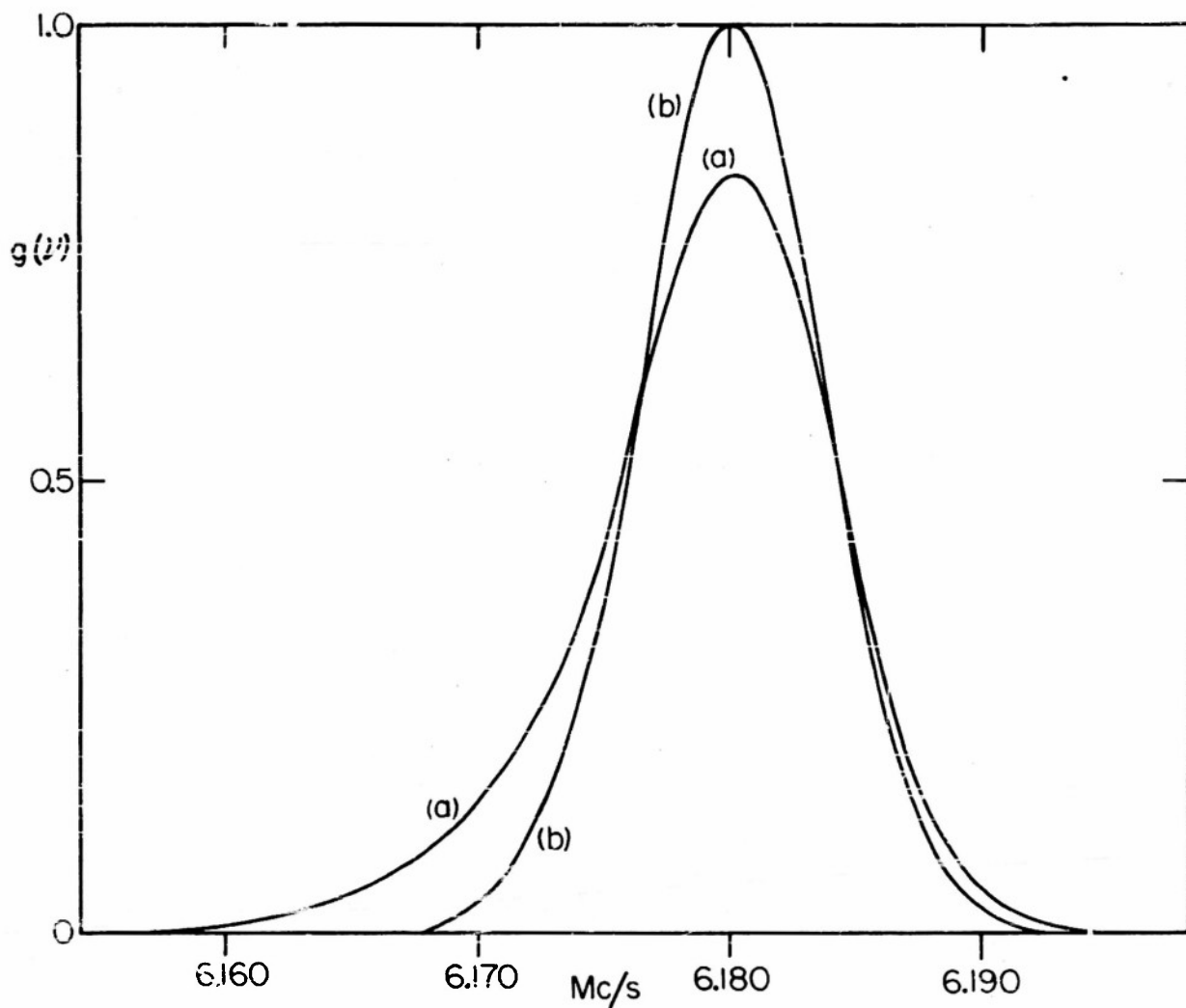


Fig. 18. (a) The shape of the  $\text{Al}^{27}$  resonance in a quenched 14 per cent Mg alloy. The line is slightly asymmetric by incipient second-order quadrupole perturbation, (b) the shape in the same sample after heat treatment. A Mg-rich phase precipitates, the signal of the Al-nuclei in the remaining matrix increases. The Mg content is still larger than 4 per cent, as the contribution from the satellites remains negligible. (Rowland).

of copper in  $\alpha$ -brass with Zn concentrations between 10 and 20 per cent would give definite information about the occurrence of ordering. Such measurements could be carried out with sufficient accuracy at liquid helium temperatures. For the completely ordered state at 25 per cent Zn the intensity drops to zero.

Although this situation cannot be realized with  $\alpha$ -brass, the same geometry is attained in  $\text{Cu}_3\text{Au}$ . The Cu atoms in this ordered cubic alloy are not centers of cubic symmetry. They have 8 Cu atoms and 4 Au atoms as nearest neighbors. Therefore the copper resonance will be unobservable in this ordered alloy. For the investigation of short-range order near the composition  $\text{Cu}_3\text{Au}$ , the  $\text{Au}^{197}$  resonance should be used. The Au atoms have a cubic environment in the ordered state. For lower Au concentrations (between 0 - 15 per cent) the copper resonance will be a suitable tool to investigate the short-range ordering in the copper-gold system.

The theory of short-range order best adapted to our problem is that of Cowley [38], who introduces a short-range order parameter for every lattice site.\* Take the origin at a copper nucleus. The probability that a site with coordinates  $\ell m n$  relative to this origin is also a copper nucleus is

$$P_{\ell mn} = 1 - C(1 - \alpha_{\ell mn})$$

where  $\alpha_{\ell mn}$  is the order parameter as defined by Cowley and C is the relative Zn concentration. Cowley shows how to obtain a set of equations for  $\alpha_i$ , the value of  $\alpha_{\ell mn}$  in the  $i^{\text{th}}$  shell around the origin, for any temperature and concentration. He gives explicit results for  $\alpha_1$ ,  $\alpha_2$  and  $\alpha_3$  for  $\text{Cu}_3\text{Au}$  as a function of temperature. These agree well with experimental X-ray data. The  $\alpha_{\ell mn}$  are the coefficients in the three-dimensional Fourier series expressing short-range order "scattering power" as a function of reciprocal-lattice coordinates. In terms of Cowley's parameters  $\alpha_1$  and  $\alpha_2$  the intensity  $g_c(\nu_{\text{max}})$  of the copper resonance in  $\alpha$ -brass becomes

$$g_c(\nu_{\text{max}}) / g_{c,o}(\nu_{\text{max}}) = (1 - C + C\alpha_1)^{12} (1 - C + C\alpha_2)^6$$

\*The author is indebted to Professor H. Brooks for calling his attention to Cowley's theory.

Here the possibility that all twelve nearest and/or six next nearest neighbors are zinc has been neglected. This method can be extended in a straightforward fashion to cases where other numbers of neighbors are involved.

### C.5 Non-cubic crystals

Finally a few remarks must be made about the influence of dislocations and other imperfections on the resonance in non-cubic single crystals and on pure quadrupole transitions.

An insulating non-cubic single crystal has a definite advantage over cubic samples in the study of quadrupole effects, because the central components and the satellites are well separated in frequency even in the perfect crystal. The broadening by imperfections can be analyzed for each line separately. The results obtained by Pound [19] on a single crystal of  $\text{Al}_2\text{O}_3$  indicate that the satellites are indeed broader than the central component, and the outer pair is again broader than the inner pair of satellites. The presence of dislocations or impurities presumably causes a distribution of  $q$ -values around the single value for the perfect crystal and the influence on each component line can be analyzed in the manner indicated above. Using equation (13) and taking for  $\lambda$  in  $\text{Al}_2\text{O}_3$  the same value as in aluminum, the density of dislocations, if these are assumed to be the cause, is estimated from Pound's recordings to be  $c \approx 3.10^7 \text{ cm}^{-2}$ .

It is not certain, however, that the broadening is only caused by a random distribution of dislocations in this non-cubic single crystal, as opposed to a previous conclusion valid for powder samples. Slightly different orientations of the axis of symmetry in various subgrains of the crystal due to dislocation walls will also produce a broadening. The magnitude of the spread in resonance frequencies caused by a distribution  $\Delta\theta$  of the angle  $\theta$  is obtained by differentiation of equation (12). A spread  $\Delta\theta$  of 0.5 degree would give the required magnitude of the broadening, which should vary as  $\sin 2\theta$ . This angular dependence is not observed experimentally, and therefore random dislocations are more likely to be the broadening agent.

In zero-field pure quadrupole spectra the presence of imperfections will cause a first-order broadening of the lines. The order of magnitude will be the same as that given by equations (13) and (16) respectively.

Pound [2] has observed such broadening due to cold work for the  $I^{127}$  pure quadrupole resonance in a molecular crystal of iodine. The  $m_I = \pm \frac{5}{2} \rightarrow \pm \frac{3}{2}$  transition is broadened twice as much as the  $m_I = \pm \frac{3}{2} \rightarrow \pm \frac{1}{2}$  transition.

#### D. Electrons

The quadrupole interaction of a nucleus with the conduction electrons does not give rise to prominent effects. In a non-cubic crystal the asymmetric charge distribution of all conduction electrons is incorporated in the distribution of all charges in the crystal to give the electric field gradient at the nucleus, and it cannot be observed separately. The asymmetric distribution of the conduction electrons near the Fermi level gives rise to an anisotropic Knight shift. The  $q_F$  of only these electrons may be observed if a nucleus with a spin  $I = \frac{1}{2}$  is present.

The quadrupole interaction will have a small effect on the relaxation time even in cubic crystals. An electron with a wave vector  $k \neq 0$  near the Fermi level can flip the nuclear spin not only by the magnetic dipolar interaction discussed previously but also by quadrupole interaction, since it has an asymmetry in its wave function and individual electrons will contribute independently to the relaxation mechanism. As the hyperfine interaction will always have a predominantly magnetic character the reduction of  $T_1$  by quadrupole interaction will be small. Nevertheless, there is some evidence from the relaxation time [16] of the isotopes  $Ga^{19}$  and  $Ga^{71}$  in metallic gallium and  $Rb^{85}$  and  $Rb^{87}$  in rubidium that quadrupole interaction contributes. The relaxation times for these isotopic pairs are not inversely proportional to the square of their gyromagnetic ratios. The relaxation time is relatively shorter for the isotopes with the larger quadrupole moment.

#### E. Phonons

The lattice vibrations will produce a time-varying gradient of the electric field even in cubic crystals. The thermal relaxation by quadrupole interaction in solids has been demonstrated in an unambiguous fashion by Pound [19] in a single crystal of sodium nitrate. His publication should be consulted for the elegant method of double resonance with simultaneous transitions at two different frequencies between the four unequally spaced levels of the  $Na^{23}$  spin. In many ionic crystals the quadrupole relaxation

is more important than the magnetic interaction via paramagnetic imperfections. The latter is the only mechanism to give reasonable relaxation time for  $I = \frac{1}{2}$ . In molecular crystals large quadrupole interactions may occur which may also determine the relaxation time. The quadrupole interaction in the presence of molecular rotation or tunnelling - which motion one may wish to consider as a special type of lattice imperfection - can be treated along the same general lines as the magnetic dipole interaction in these cases. Most of the experimental work concerned with this type of thermal motion has been done for protons, for which the quadrupole interaction is of course absent. Diffusion in solids and quadrupole relaxation has already been discussed earlier in this review.

#### F. Excitons

No information of either theoretical or experimental nature of the quadrupole interaction around these imperfections is known to the author. It is doubtful whether they can be produced in sufficient concentration to cause observable effects.

This survey may be terminated with these concluding remarks. The influence of imperfections on nuclear magnetic resonance signals is frequently so profound that inversely the magnetic resonance may be used as a tool for the investigation of the nature of the imperfections. In general, the quadrupole effects are more pronounced than the magnetic effects. Problems which can be attacked successfully with nuclear resonance techniques include: self-diffusion, ionic diffusion, electronic structure of metals and alloys, density of bound and free carriers in semiconductors, magnetic properties of F-centers, density and distribution of dislocations, density and distribution of vacancies and interstitials, lattice deformation and electron distribution around chemical impurities, short-range order, precipitation and radiation damage. The application of nuclear resonance techniques to these fields has only just started. This review should therefore be considered as a progress report. Many new results are likely to be obtained in the near future.

### Acknowledgment

The author is indebted to Professor H. Brooks and Professor R. V. Pound for reading the manuscript and several valuable discussions.

### References

1. F. Seitz, Imperfections in Nearly Perfect Crystals, edited by Shockley et al., John Wiley, New York, 1952.
2. R. V. Pound, J. Phys. Chem. 57, 743 (1953).
3. J. H. Van Vleck, Phys. Rev. 74, 1168 (1948).
4. N. Bloembergen, E. M. Purcell and R. V. Pound, Phys. Rev. 73, 678 (1948).
5. H. C. Torrey, Phys. Rev. 92, 962 (1953).
6. C. P. Slichter and R. E. Norberg, Phys. Rev. 83, 1074 (1951).  
H. S. Gutowski, Phys. Rev. 83, 1073 (1951).
7. N. Bloembergen, Physica 15, 386 (1949).
8. B. V. Rollin and J. Hatton, Phys. Rev. 74, 346 (1948). R. V. Pound, Phys. Rev. 81, 156 (1951).
9. W. D. Knight, Phys. Rev. 76, 1259 (1949).
10. C. H. Townes, C. Herring and W. D. Knight, Phys. Rev. 77, 852 (1950).
11. N. Bloembergen and T. J. Rowland, Acta Met. 1, 731 (1953).
12. N. F. Mott and H. Jones, Properties of Metals and Alloys, p. 87, Oxford University Press, 1936.
13. J. Friedel, Phil. Mag. 43, 153 (1952).
14. N. Bloembergen, Physica, Proceedings of the Semiconductor Conference, Amsterdam, 1954.
15. J. Korringa, Physica 16, 601 (1950).
16. H. S. Gutowski and B. R. McGarvey, J. Chem. Phys. 20, 1472 (1952).
17. I. Waller, Z. Phys. 79, 370 (1950).

18. R. V. Pound, *Progress in Nuclear Physics* 2, 21 (1952), and other references quoted in this review article.
19. R. V. Pound, *Phys. Rev.* 79, 685 (1950).
20. G. M. Volkoff, *Can. J. Phys.* 31, 820 (1953).
21. B. T. Feld and W. E. Lamb, *Phys. Rev.* 67, 15 (1945).
22. W. A. Nierenberg and N. F. Ramsey, *Phys. Rev.* 72, 1075 (1947).
23. H. G. Dehmelt, *Am. J. Phys.* 22, 110 (1954).
24. G. D. Watkins and R. V. Pound, *Phys. Rev.* 89, 658 (1953). G. D. Watkins, Thesis, Harvard University, 1952 (unpublished).
25. H. M. Foley, R. M. Sternheimer and D. Tycke, *Phys. Rev.* 93, 734 (1954).
26. A. H. Cottrell, *Dislocations and Plastic Flow in Crystals*, p. 34, Oxford, 1953.
27. P. Gay, P. B. Hirsch and A. Kelly, *Acta Met.* 1, 315 (1953). A. H. Cottrell, loc. cit. pp. 100 ff.
28. See, for example, A. H. Cottrell, loc. cit. pp. 152 ff.
29. K. Kambe, private communication (to be published).
30. N. Bloembergen, *Nuclear Magnetic Relaxation*, Thesis, Leiden (1948).
31. R. V. Pound, *Phys. Rev.* 72, 1273 (1947).
32. A. E. H. Love, *Theory of Elasticity*, p. 142, Cambridge, 1927. S. Timoshenko, *Theory of Elasticity*, p. 323, McGraw-Hill, New York, 1934.
33. A. B. Lidiard, *Phys. Rev.* 94, 29 (1954).
34. F. Reif, private communication. M. Cohen, *Proceedings of the Bristol Conference*, 1954.
35. T. J. Rowland, (to be published). T. J. Rowland, Thesis, Harvard University, 1954 (unpublished).
36. A. H. Cottrell, *Progress in Metal Physics* I, Butterworth, London, 1949.
37. W. Hume-Rothery, *The Structure of Metal and Alloys*, The Institute of Metals Report 1, London, 1936.
38. J. M. Cowley, *Phys. Rev.* 77, 669 (1950).
39. J. P. Lloyd and G. E. Pake, *Phys. Rev.* 94, 579 (1954).

### Appendix

It has been shown early in the history of nuclear magnetic relaxation [30] that the relaxation of a spin system with  $2I + 1$  equidistant levels has the following characteristics.

The saturation under the influence of a steady-state radio-frequency field is given by

$$\chi''/\chi''_0 = \Delta n/\Delta n_0 = [1 + \frac{1}{4} \gamma^2 H_{rf}^2 T_1 g(\nu)]^{-1}$$

where  $\Delta n$  is the difference in population between adjacent levels in the presence of an oscillating field with rms amplitude  $H_{rf}$  and  $\Delta n_0$  the difference under thermal equilibrium in the absence of the rf field. The recovery of the system to the state of thermal equilibrium after the rf field has been turned off is given by a simple exponential function with characteristic time  $T_1$ .

Whenever the splitting of the spin levels is non-equidistant the problem of relaxation becomes rather complicated. The steady-state condition can still be analyzed readily in terms of the population number of each level, if the establishment of spin-spin equilibrium in each level is more rapid than the spin-lattice relaxation. Pound [19] has discussed this situation for systems with quadrupole coupling and Pake [39] for the case of magnetic hyperfine splittings. The transitions between the different energy levels may have different saturation parameters. The recovery is now a rather complicated process and is not related to the steady-state saturation in the simple manner as it was for equidistant levels. In the case of quadrupole interaction in metals the recovery can be analyzed in detail. We shall describe the situation which applies to cold-worked copper ( $I = \frac{3}{2}$ ). The external field produces transitions only between the levels  $m_I = \frac{1}{2}$  and  $-\frac{1}{2}$ . The relaxation process is entirely due to interaction with the conduction electrons which produces transitions between adjacent nuclear spin levels only. The transition probability per unit time between the levels  $m$  and  $m - 1$  is

$$w = 2\pi \gamma^2 \rho_{th}(\nu) (I+m)(I-m+1) = (2T_1)^{-1} (I+m)(I-m+1)$$

It is independent of the quadrupole splitting, as the conduction electrons take up any small energy balance in their kinetic energy;  $\rho_{in}(\nu)$  is constant up to very high frequencies.  $T_1$  is the relaxation time in well-annealed copper where the levels are equidistant. The differential equations describing the relaxation process are

$$\frac{dn_{3/2}}{dt} = + \frac{3}{2T_1} (-n_{3/2} + n_{3/2}^0 + n_{1/2} - n_{1/2}^0)$$

$$\frac{dn_{1/2}}{dt} = - \frac{dn_{3/2}}{dt} + \frac{2}{T_1} (-n_{1/2} + n_{1/2}^0 + n_{-1/2} - n_{-1/2}^0) + \gamma^2 H_{rf}^2 (-n_{1/2} + n_{-1/2}) g(\nu)$$

$$\frac{dn_{-1/2}}{dt} = - \frac{dn_{-3/2}}{dt} - \frac{dn_{1/2}}{dt} - \frac{dn_{3/2}}{dt}$$

$$\frac{dn_{-3/2}}{dt} = - \frac{3}{2T_1} (-n_{-3/2} + n_{-3/2}^0 + n_{-1/2} - n_{-1/2}^0)$$

The third equation could of course be written in a form symmetrical to the second, but it shows clearly the obvious relation that the total number of spins  $n_{3/2} + n_{1/2} + n_{-1/2} + n_{-3/2}$  remains constant. It is easily verified that under steady-state conditions the same saturation relation is still satisfied. Except for the small change in  $g(\nu)$  due to quadrupole splitting, the nuclear signal in cold-worked copper will saturate at the same power level as in annealed copper.

The recovery time after saturation of the central transition is different. For  $H_{rf} = 0$  the system of equations reduces to two independent linear differential equations for  $n_{1/2} - n_{-1/2}$  and  $n_{3/2} - n_{-3/2}$  with the solution

$$n_{1/2} - n_{-1/2} = A \exp(-t/T_1) + B \exp(-6t/T_1) + n_{1/2}^0 - n_{-1/2}^0$$

The constants A and B are determined from the initial conditions at  $t = 0$ ,

$$n_{1/2} - n_{-1/2} = 0 \text{ and } n_{3/2} - n_{-3/2} = n_{3/2}^0 - n_{-3/2}^0 - n_{1/2}^0 + n_{-1/2}^0 \text{ or } \frac{d}{dt} (n_{3/2} - n_{-3/2}) = 0$$

The result is then the equation used in the text,

$$\Delta n = \left\{ -\frac{2}{5} \exp(-t/T_1) - \frac{3}{5} \exp(-6t/T_1) + 1 \right\} \Delta n_0$$

Pulse techniques which measure these transient effects should therefore give different results in the cold-worked material from steady-state techniques, unless the pulses are of such short duration and consequently their frequency spectra so wide that they turn all spins rather than change the magnetization of the central states  $m_I = \frac{1}{2}$  or  $-\frac{1}{2}$  only.

If the dominant relaxation mechanism is caused by dipolar interaction between pairs of nuclear dipoles, the set of differential equations becomes non-linear and would not permit a solution in closed form. It can, however, be linearized by assuming that the population of any of the  $2I + 1$  levels never deviates much from  $N/(2I + 1)$ . Introduce the deviation  $\Delta n_m$  and neglect products of these small quantities. In the case of quadrupole relaxation the system remains linear in the population numbers  $n$  and a solution for transients can be obtained in principle. The relation to the steady-state solution will be different in each individual case.

## DISTRIBUTION LIST

### Technical Reports

2	Chief of Naval Research (427) Department of the Navy Washington 25, D. C.
1	Chief of Naval Research (460) Department of the Navy Washington 25, D. C.
1	Chief of Naval Research (421) Department of the Navy Washington 25, D. C.
6	Director (Code 2000) Naval Research Laboratory Washington 25, D. C.
2	Commanding Officer Office of Naval Research Branch Office 150 Causeway Street Boston, Massachusetts
1	Commanding Officer Office of Naval Research Branch Office 1000 Geary Street San Francisco 9, California
1	Commanding Officer Office of Naval Research Branch Office 1030 E. Green Street Pasadena, California
1	Commanding Officer Office of Naval Research Branch Office The John Crerar Library Building 86 East Randolph Street Chicago 1, Illinois
1	Commanding Officer Office of Naval Research Branch Office 346 Broadway New York 13, New York
3	Officer-in-Charge Office of Naval Research Navy No. 100 Fleet Post Office New York, N. Y.

1 Chief, Bureau of Ordnance (Re 4)  
Navy Department  
Washington 25, D. C.

1 Chief, Bureau of Ordnance (AD-3)  
Navy Department  
Washington 25, D. C.

1 Chief, Bureau of Aeronautics (EL-1)  
Navy Department  
Washington 25, D. C.

2 Chief, Bureau of Ships (810)  
Navy Department  
Washington 25, D. C.

1 Chief of Naval Operations (Op-413)  
Navy Department  
Washington 25, D. C.

1 Chief of Naval Operations (Op-20)  
Navy Department  
Washington 25, D. C.

1 Chief of Naval Operations (Op-32)  
Navy Department  
Washington 25, D. C.

1 Director  
Naval Ordnance Laboratory  
White Oak, Maryland

2 Commander  
U. S. Naval Electronics Laboratory  
San Diego, California

1 Commander (AAEL)  
Naval Air Development Center  
Johnsville, Pennsylvania

1 Librarian  
U. S. Naval Post Graduate School  
Monterey, California

50 Director  
Signal Corps Engineering Laboratories  
Evans Signal Laboratory  
Supply Receiving Section  
Building No. 42  
Belmar, New Jersey

- 3           **Commanding General (RDRRF)**  
            **Air Research and Development Command**  
            **Post Office Box 1395**  
            **Baltimore 3, Maryland**
- 2           **Commanding General (RDDDE)**  
            **Air Research and Development Command**  
            **Post Office Box 1395**  
            **Baltimore 3, Maryland**
- 1           **Commanding General (WCRR)**  
            **Wright Air Development Center**  
            **Wright-Patterson Air Force Base, Ohio**
- 1           **Commanding General (WCRRH)**  
            **Wright Air Development Center**  
            **Wright-Patterson Air Force Base, Ohio**
- 1           **Commanding General (WCRE)**  
            **Wright Air Development Center**  
            **Wright-Patterson Air Force Base, Ohio**
- 2           **Commanding General (WCRET)**  
            **Wright Air Development Center**  
            **Wright-Patterson Air Force Base, Ohio**
- 1           **Commanding General (WCREO)**  
            **Wright Air Development Center**  
            **Wright-Patterson Air Force Base, Ohio**
- 2           **Commanding General (WCLR)**  
            **Wright Air Development Center**  
            **Wright-Patterson Air Force Base, Ohio**
- 1           **Commanding General (WCLRR)**  
            **Wright Air Development Center**  
            **Wright-Patterson Air Force Base, Ohio**
- 2           **Technical Library**  
            **Commanding General**  
            **Wright Air Development Center**  
            **Wright-Patterson Air Force Base, Ohio**
- 1           **Commanding General (RCREC-4C)**  
            **Rome Air Development Center**  
            **Griffiss Air Force Base**  
            **Rome, New York**
- 1           **Commanding General (RCR)**  
            **Rome Air Development Center**  
            **Griffiss Air Force Base**  
            **Rome, New York**

- 2            Commanding General (RCRW)  
             Rome Air Development Center  
             Griffiss Air Force Base  
             Rome, New York
- 6            Commanding General (CRR)  
             Air Force Cambridge Research Center  
             230 Albany Street  
             Cambridge 39, Massachusetts
- 1            Commanding General  
             Technical Library  
             Air Force Cambridge Research Center  
             230 Albany Street  
             Cambridge 39, Massachusetts
- 2            Director  
             Air University Library  
             Maxwell Air Force Base, Alabama
- 1            Commander  
             Patrick Air Force Base  
             Cocoa, Florida
- 2            Chief, Western Division  
             Air Research and Development Command  
             P. O. Box 2035  
             Pasadena, California
- 1            Chief, European Office  
             Air Research and Development Command  
             Shell Building  
             60 Rue Ravenstein  
             Brussels, Belgium
- 1            U. S. Coast Guard (EEE)  
             1300 E Street, N. W.  
             Washington, D. C.
- 1            Assistant Secretary of Defense  
             (Research and Development)  
             Research and Development Board  
             Department of Defense  
             Washington 25, D. C.
- 5            Armed Services Technical Information Agency  
             Document Service Center  
             Knott Building  
             Dayton 2, Ohio

- 1            Director  
            Division 14, Librarian  
            National Bureau of Standards  
            Connecticut Avenue and Van Ness St., N. W.
- 1            Director  
            Division 14, Librarian  
            National Bureau of Standards  
            Connecticut Avenue and Van Ness St., N. W.
- 1            Office of Technical Services  
            Department of Commerce  
            Washington 25, D. C.
- 1            Commanding Officer and Director  
            U. S. Underwater Sound Laboratory  
            New London, Connecticut
- 1            Federal Telecommunications Laboratories, Inc.  
            Technical Library  
            500 Washington Avenue  
            Nutley, New Jersey
- 1            Librarian  
            Radio Corporation of America  
            RCA Laboratories  
            Princeton, New Jersey
- 1            Sperry Gyroscope Company  
            Engineering Librarian  
            Great Neck, L. I., New York
- 1            Watson Laboratories  
            Library  
            Red Bank, New Jersey
- 1            Professor E. Weber  
            Polytechnic Institute of Brooklyn  
            99 Livingston Street  
            Brooklyn 2, New York
- 1            University of California  
            Department of Electrical Engineering  
            Berkeley, California
- 1            Dr. E. T. Booth  
            Hudson Laboratories  
            145 Palisade Street  
            Dobbs Ferry, New York
- 1            Cornell University  
            Department of Electrical Engineering  
            Ithaca, New York

- 1 University of Illinois  
Department of Electrical Engineering  
Urbana, Illinois
- 1 Johns Hopkins University  
Applied Physics Laboratory  
Silver Spring, Maryland
- 1 Professor A. von Hippel  
Massachusetts Institute of Technology  
Research Laboratory for Insulation Research  
Cambridge, Massachusetts
- 1 Director  
Lincoln Laboratory  
Massachusetts Institute of Technology  
Cambridge 39, Massachusetts
- 1 Signal Corps Liaison Office  
Massachusetts Institute of Technology  
Cambridge 39, Massachusetts
- 1 Mr. Hewitt  
Massachusetts Institute of Technology  
Document Room  
Research Laboratory of Electronics  
Cambridge, Massachusetts
- 1 Stanford University  
Electronics Research Laboratory  
Stanford, California
- 1 Professor A. W. Straiton  
University of Texas  
Department of Electrical Engineering  
Austin 12, Texas
- 1 Yale University  
Department of Electrical Engineering  
New Haven, Connecticut
- 1 Mr. James F. Trosch, Administrative Aide  
Columbia Radiation Laboratory  
Columbia University  
538 West 120th Street  
New York 27, N. Y.
- 1 Dr. J. V. N. Granger  
Stanford Research Institute  
Stanford, California

# Armed Services Technical Information Agency

Because of our limited supply, you are requested to return this copy WHEN IT HAS SERVED YOUR PURPOSE so that it may be made available to other requesters. Your cooperation will be appreciated.

# AD

# 40603

NOTICE: WHEN GOVERNMENT OR OTHER DRAWINGS, SPECIFICATIONS OR OTHER DATA ARE USED FOR ANY PURPOSE OTHER THAN IN CONNECTION WITH A DEFINITELY RELATED GOVERNMENT PROCUREMENT OPERATION, THE U. S. GOVERNMENT THEREBY INCURS NO RESPONSIBILITY, NOR ANY OBLIGATION WHATSOEVER; AND THE FACT THAT THE GOVERNMENT MAY HAVE FORMULATED, FURNISHED, OR IN ANY WAY SUPPLIED THE SAID DRAWINGS, SPECIFICATIONS, OR OTHER DATA IS NOT TO BE REGARDED BY IMPLICATION OR OTHERWISE AS IN ANY MANNER LICENSING THE HOLDER OR ANY OTHER PERSON OR CORPORATION, OR CONVEYING ANY RIGHTS OR PERMISSION TO MANUFACTURE, USE OR SELL ANY PATENTED INVENTION THAT MAY IN ANY WAY BE RELATED THERETO.

Reproduced by  
**DOCUMENT SERVICE CENTER**  
KNOTT BUILDING, DAYTON, 2, OHIO

# UNCLASSIFIED